Appendix C

"Flight Test Analysis of the Forces and Moments Imparted on a Boeing 737-100 Airplane During Wake-Vortex Aircraft Encounters"

A Maters Thesis

Submitted to

the Department of Mechanical Engineering

Howard University

April 12, 2001

Note: This is a draft copy; the final corrected version has not been received from the student.

Dr. Sonya T. Smith
Howard University

HOWARD UNIVERSITY

FLIGHT TEST ANALYSIS OF THE FORCES AND MOMENTS IMPARTED ON A B737-100 AIRPLANE DURING WAKE VORTEX ENCOUNTERS

*

A Thesis
Submitted to the Faculty of the
Graduate School of Arts and Sciences

of

HOWARD UNIVERSITY

in partial fulfillment of
the requirements for the
degree of

Master of Engineering in Mechanical Engineering

Department of Mechanical Engineering

by

Christopher L. Roberts

*

Washington, D.C.
April 12, 2001

HOWARD UNIVERSITY
GRADUATE SCHOOL OF ARTS AND SCIENCES
DEPARTMENT OF MECHANICAL ENGINEERING

THESIS COMMITTEE

Robert Reiss, Ph.D.
Committee Chairman

Sonya T. Smith, Ph.D.
Thesis Advisor

Arthur Thorpe, Ph.D.

Dan D. Vicroy
External Examiner
NASA LaRC

Sonya T. Smith, Ph.D.
Thesis Advisor

Candidate: Christopher L. Roberts

Date of Defense: April 12, 2001

ACKNOWLEDGEMENTS

I would like to thank Dr. Sonya Smith for her patience, support, and consistent motivation throughout this process. I would also like to thank Dan D. Vicroy and NASA LaRC Research Center. I would also like to thank the Department of Mechanical Engineering and the Center for the Study of Terrestrial and Extraterrestrial Atmospheres.

ABSTRACT

Aircraft travel has become a major form of transportation. Several of our major airports are operating near their capacity limit, increasing congestion and delays for travelers. As a result, the National Aeronautics and Space Administration (NASA) has been working in conjunction with the Federal Aviation Administration (FAA), airline operators, and the airline industry to increase airport capacity without sacrificing public safety. One solution to the problem is to increase the number of airports and build new runways; yet, this solution is becoming increasingly difficult due to limited space. A better solution is to increase the production per runway. This solution increases the possibility that one aircraft will encounter the trailing wake of another aircraft. Hazardous wake vortex encounters occur when an aircraft encounters the wake produced by a heavier aircraft. This heavy-load aircraft produces high-intensity wake turbulence that redistributes the aerodynamic loads of trailing smaller aircraft. This situation is particularly hazardous for smaller aircraft during takeoffs and landings.

In order to gain a better understanding of the wake-vortex/aircraft encounter phenomena, NASA Langley Research Center conducted a series of flight tests from 1995 through 1997. These tests were designed to gather data for the development a wake encounter and wake-measurement data set with the accompanying atmospheric state information. This data set is being compiled into a database that can be used by wake vortex researchers to compare with experimental and computational results. The purpose of this research is to derive and implement a procedure for calculating the wake-vortex/aircraft interaction portion of that database by using the data recorded during those flight tests.

There were three objectives to this research. Initially, the wake-induced forces and moments from each flight were analyzed based on varying flap deflection angles. The flap setting alternated between 15 and 30 degrees while the separation distance remained constant. This examination was performed to determine if increases in flap deflection would increase or decrease the effects of the wake-induced forces and moments. Next, the wake-induced forces and moments from each flight were analyzed based on separation distances of 1-3 nautical miles. In this comparison, flap deflection was held constant at 30 degrees. The purpose of this study was to determine if increased separation distances reduced the effects of the wake vortex on the aircraft. The last objective compared the wake-induced forces and moments of each flight as it executed a series of maneuvers through the wake-vortex. This analysis was conducted to examine the impact of the wake on the B737 as it traversed the wake horizontally and vertically.

Results from the first analysis indicated that there was no difference in wake effect at flap deflections of 15 and 30 degrees. This conclusion is evidenced in the cases of the wake-induced sideforce, rolling moment, and yawing moment. The wake–induced lift, drag, and pitching moment cases yielded less conclusive results. The second analysis compared the wake-induced forces and moments at separation distances of 1-3 nautical miles. Results indicated that there was no significant difference in the wake-induced lift, drag, sideforce, or yawing moment coefficients. The analysis compared the wake-induced forces and moments based on different flight maneuvers. It was found that the wake-induced forces and moments had the greatest impact on out-to-in and in-to-out maneuvers.

LIST OF SYMBOLS

Acc	acceleration, ft/sec^2
b	wing span, ft
c	wing chord, ft
C_D	drag coefficient
C_l , C_{LS}	rolling moment coefficient
C_L	lift coefficient
C_M	pitching moment coefficient
C_N	yawing moment coefficient
C_Y	sideforce coefficient
F_{NZ}	normal direction acceleration, ft/sec^2
g	acceleration due to gravity, ft/sec^2
H	altitude, ft
Mach	Mach number, Mach
P	roll rate, deg/sec
Press	static pressure, lbs/ft^2
Q	pitch rate, deg/sec
q	dynamic pressure, lbs/ft^2
R	yaw rate, deg/sec
S	wing surface area, ft^2
T	time, sec
T_{AS}	true airspeed, knots
T_{EMP}	temperature, °C
T_m	thrust contribution in the pitching moment
T_n	thrust contribution in the yawing moment
T_X	thrust body axis thrust
U_B	aircraft longitudinal velocity in the body axis, ft/s
V_B	aircraft lateral velocity in the body axis, ft/s
W_B	aircraft vertical velocity in the body axis, ft/s
V_{WND}	wind speed, knots
W	weight, lbs
W_E	east wind velocity component in the Earth axis system, ft/s
W_N	north wind velocity component in the Earth axis system, ft/s
W_Z	vertical wind velocity component in the Earth axis system, ft/s
X	longitudinal axis
x	coordinate along X axis, ft
y	coordinate along Y axis, ft
Y	lateral axis
z	coordinate along Z axis, ft
Z	vertical axis
α	angle of attack, deg
β	sideslip angle, deg
θ	pitch angle, deg

ϕ	roll angle, deg
Ψ	true heading, deg
δ	deflection

Subscripts

A	aileron position, deg
B	reference to body axis system
bias	flight data bias
E	East direction
ELEV	elevator position
E.O.M	equations of motion
EPR1	engine pressure ratio of engine 1, epr
EPR2	engine pressure ratio of engine 2, epr
Flap	flap position, deg
LG	landing gear position (Down =1, Up =2)
Lat	lateral
Lon	longitudinal
M.bias	mean flight data bias
N	North direction
no wake	out of the presence of the wake
R	rudder deflection, deg
Stab	horizontal stabilizer deflection, deg
SPL	left spoiler deflection, deg
SPR	right spoiler deflection, deg
wake	in the presence of the wake
wi	wake-induced component
WND	wind
Z	Vertical or down direction

Abbreviations

AC	aircraft
ATC	Air Traffic Controller
FAA	Federal Aviation Administration
FAM	forces and moments
IFR	Instrument Flight Regulations
LaRC	Langley Research Center
NASA	National Aeronautics and Space Administration
VFR	Visual Flight Regulations

TABLE OF CONTENTS

LIST OF TABLES

LIST OF FIGURES

CHAPTER 1: INTRODUCTION

1.1 Purpose of Study

Aircraft travel has been a primary form of transportation over the past four decades. Due to increased air traffic, major airports are currently operating at or near their capacity limit. This has translated into increased congestion and passenger delay. As early as the 1950s, scientists have recognized this as a potential problem and sought methods to alleviate this condition. Recently, the National Aeronautics and Space Administration (NASA) has been working in conjunction with the Federal Aviation Administration (FAA), commercial airlines, and aircraft manufactures to increase airport capacity and improve safety. Several solutions have been proposed. The most feasible method is to increase the production per runway by decreasing the separation distances between aircraft during takeoffs and landings during instrument flight rules.

Depending upon the flight airspace, weather, visibility, and the aircraft's distance from clouds, Air Traffic Regulations require pilots to fly under either Visual Flight Rules (VFR) or Instrument Flight Rules (IFR). Under VFR, the pilots are responsible for maintaining safe separation distances. Under IFR, Air Traffic Controllers (ATC) are responsible for maintaining the separation distances mandated by the FAA [1]. When conditions require an airport to operate under IFR, the airport capacity is significantly diminished. This has led to speculation that IFR separation may unnecessarily limit the operating capacity of major airports.

In order to decrease IFR separation distances, it is necessary to address the issue of a hazardous wake encounter. Wake vortices, also known as wing-tip vortices, are created

when the airflow over the top surface of a wing meets the airflow over the top of the bottom wing surface. The air flowing over the top surface of the wing flows inwards towards the wing centerline; whereas, the air flowing over the under-surface of the wing flows outward towards the wing's tip. When the two airflows meet at the wing's trailing edge, they join at an angle creating counter rotating vortices.

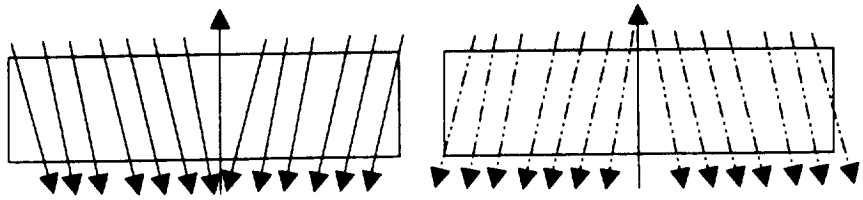

Figure 1: Wake formation process

Vortices are created by all classes of aircraft: Heavy (300,000lb or more), Large (between 12,500lb and 300,000lb), and Small (less than 12,500lb) [3]. When a following, small-load aircraft encounters the wake from a heavy-load aircraft, the aerodynamic load of the following aircraft is redistributed. This can result in a loss of control for the smaller aircraft and is particularly hazardous during take-offs and landings. For this reason, the FAA has set specific longitudinal separation distance guidelines to avoid wake-vortex encounters(Table 1).

Following Aircraft	Leading Aircraft		
	HEAVY	LARGE	SMALL
HEAVY	4	3	3
LARGE	5	3	3
SMALL	6	4	3

Table 1: U.S. Wake-Vortex Separation Standards, in nautical miles.

As more and more airplanes are placed into the terminal area, the probability of encountering a trailing wake-vortex is increased. Therefore, a better understanding of wake-vortex/aircraft interactions has to be gained before new separation guidelines can be established.

The purpose of this project is to design and implement a procedure for computing the wake-induced forces and moments imparted on an aircraft during a wake-vortex encounter. The author conducted research at NASA Langley Research Center utilizing data that was collected in a series of flight tests from 1995-1997. Information gathered in this study will be stored in a comprehensive database containing wake-vortex, atmospheric state, and wake-vortex/aircraft encounter data. The database will then be used for the comparison and validation of current and future wake-encounter simulations. Such simulation data can be used by the FAA to evaluate reduced separation guidelines.

1.2 Literature Review

Current separation distances were derived in the 1960's and 1970's using simulations consisting of simple wake vortex models (one-degree-of-freedom roll upset models, strip models, vortex-lattice models, simplified Navier-Stokes solutions, etc.) [1].
At that time, there was a lack of adequate flight tests or wind tunnel data; therefore, primary validation of these simulations was from pilot subjective evaluations [2]. These comments were little more than remarks that each pilot made concerning the accuracy of the simulation based on their wake encounter flight experience. These separation guidelines may be overly conservative since the reduced separations under Visual Flight Rules (VFR) operations have not resulted in an increase in wake encounters. For this reason, additional research has been

conducted into wake vortices and the wake-vortex/ aircraft interaction with hopes of ultimately reducing the separation distance guidelines.

Greene [5] studied the effects of the atmosphere on wake-vortex motion and decay at ground facilities. He combined the effects of the Reynold's number, density stratification, and turbulence in one model which estimated the influence of these direct parameters on wake lifetimes and decay. Greene's model agreed well with ground and facility tests in terms of density stratification. The Reynolds number had a relatively small effect on wake decay, but could partially explain the differences in wake lifetimes between ground and facility tests. The model data also concluded that the wake lifetimes could be less than the FAA mandated separation times by a scale factor of approximately two or three. This situation seemed to be true under conditions of strong stratification, turbulence or both. Similarly, Corjon et. al. [6] modified Greene's model to take into account ground effects (divergence, rebound) and crosswind (advection, shear). This model showed that the minimum longitudinal separations could be reduced under the particular meteorological conditions of strong crosswind and shear.

Janota et. al. [7] used the most complete wake vortex and weather data to relate the lifetimes and decent distances of vortices to measured and derived aircraft variables. These vortices were also compared to atmospheric variables. The purpose was to look for physical relationships and determine the viability of predicting vortex behavior from independent data. The model used in this study was a multiple linear regression (MLR) model. Atmospheric data was obtained from an instrument tower and a tethersonde. The wake-vortex data came from a series of low level airliner flybys using a lidar scanner. This wake vortex data set, as well as the MLR models, seemed to support the observation that vortex

lifetimes were shortened due to turbulence created by daytime convective heating. The wake vortices tended to descend further in the early morning hours when the temperature was cooler. It was found that strong predictors of vortex lifetimes were total wind speed and crosswind.

Ash et. al. [8] also studied the effects of crosswind on turbulent wake vortices near the ground. A Reynolds stress transport turbulence model was used to simulate the two dimensional behavior of the aircraft wake vortices and atmospheric turbulence was calculated using stream function-vorticity numerical formulation. This model was later modified to include the mean crosswind and ambient turbulence. The results of the simulation showed that the ambient turbulence accelerated the rate of vortex decay. It was determined that atmospheric turbulence effects negate the wake vortex hazard when the crosswind level is above the limits for a safe aircraft landing.

In addition to studying wake vortex behavior and decay as a result of different atmospheric factors, a great deal of research has been dedicated to studying the wake-vortex encounter hazard. Sammonds et. al. [9] studied the criteria relating the wake vortex encounter hazard to an aircraft response. The primary objectives of the study were to validate the ability of simulators to produce realistic wake vortex encounters and determine the hazard criteria in terms of aircraft responses for two classes of aircraft. A six degree-of-freedom piloted simulator was used to study the wake vortex encounter hazard for small and heavy aircraft (Learjet and a Boeing 707/720). Validation for the simulator was based on the assessment of four pilots. These pilots gave the simulation a favorable evaluation; they cited that the simulation and the vortex encounters seemed realistic. They determined that the primary motion, which was about the roll axis, was highly realistic. The study also found the

parameter that predicted the best hazard boundary was roll angle, the angle at which the aircraft turns with respect to horizontal. Other research supported this conclusion, stating that the wake-vortex induced rolling moment coefficient was the most important of all the components of forces and moments [10].

Stuever et al. [11] performed a similar study some years later. In this study, a one-degree-of-freedom roll axis model was used to find the wake upset hazards. The wake-upset criterion was defined as a boundary of allowable vortex-induced bank angle versus altitude. This bank angle was defined as the angle imposed on the aircraft due to the wake vortex. Results of this study showed that the separation distance was strongly dependent on the atmospheric conditions.

Stewart [12] also performed an analytical study of the interaction between a wake vortex and an encountering, following airplane. He conducted tests to address the effect of two assumptions made on simulated aircraft responses. The two assumptions were that all of the angular momentum was absent from the vortex before the trailing aircraft encountered it and that the encountering aircraft was only influenced by the wake-vortex directly in front of it. For this reason, a single vortex was used to model the wake vortex and the following plane was assumed to consist only of a wing. Thus, a numerical simulation of a one degree-of-freedom encounter was thus developed to measure the aircraft's motions. Formulas were also developed to calculate the rolling moment on the plane and the angular momentum of a cylindrical section of a vortex with a tapered core. In studying the three different categories of planes, it was determined that the amount of angular momentum in the wake available for transfer to the following plane was large. Results of the study also indicated that the majority of angular momentum in the vortex was in the regions farthest from the core.

Another study conducted by Walden et. al. [13] looked at the wake-induced forces and moments imposed on a business jet configuration. The model used a low-order potential-flow panel method called PMARC. The unique feature of PMARC was that it had two options: a user-specified rigid wake and an unsteady, or time dependent, wake feature. While the rigid wake option had the benefit of being aligned with the freestream velocity, the unsteady wake option provided the ability to stop the wake with the local velocity. Comparisons between the PMARC data and wind tunnel data revealed that PMARC could predict forces and moments with acceptable accuracy.

Brandon et. al. [14] performed wind tunnel studies to access the feasibility of using free-flight testing techniques to study wake vortex encounters. In NASA Langley Research Center's (LaRC) 30 x 60 wind tunnel, a remotely controlled dynamically scaled model was flown in the wake of a vortex generating wing. The wing, fitted with smoke-tip generators, was mounted in the forward section of the wind tunnel. The angle of attack of the wing was also varied to enable the selection of vortex strength. The vortical flow field produced various rolling moments on the model. As expected, these moments were found to be dependent upon the vortex strength and the relative position of the model. Overall, the study showed that the free-flight test technique was a viable means of studying wake-vortex/aircraft encounters.

Vicroy et. al.[15] also published a series of papers detailing NASA LaRC's efforts to study aircraft/wake vortex interactions. In one study, a Boeing 737-100 simulation was used to define the wake decay required for the B737 to safely encounter a B727. The simulation was modified to include a wake model and a strip-theory model to calculate the forces and moments. Input to the simulation came from an autoland system rather than the pilot.

While the results of that simulation are still being studied, preliminary results indicate that the roll, or bank, angle was the dominant limiting criteria for altitudes of above 150 feet. Below 150 feet, the horizontal boundary was the only limiting factor.

In another study, Stuever et, al. [16] described recent flight testing methods to obtain a detailed wake development data set. A highly instrumented Rockwell OV-10A was flown into the wake generated by a Lockheed Martin C-130. The OV-10 measured the wake velocities and ambient weather conditions related to wake transport and decay. The OV-10A was also equipped with a stereo—photographic imaging system, which enabled researchers to measure the various wake characteristics. Over the course of seven flights, the OV-10 measured the wake by flying slower than the C-130 and making a series of wake penetrations. The purpose of the data collected was to integrate all relevant flight data into an organized and structured database [17]. The database will then be used to determine aircraft-to-vortex distances for vortex characterization and vortex-encounter flights.

The study of trailing wakes it not a new issue. Researchers have studied them for decades in an attempt to understand the dynamics of interaction with an encountering aircraft. If new separation distances are to be established, then acceptable and hazardous wake-vortex/aircraft encounter metrics have to be determined. The only means of doing this is by developing an accurate and validated means of studying the wake-vortex effects on an aircraft.

1.3 Contribution

As stated in section 1.2, various laboratory experiments and analytical models have been developed to study the dynamics of wake-vortex/aircraft encounters as well as wake-vortex flow physics. However, there is very little comprehensive data available for comparison and/or validation of the experimental and computational results. Many of the previous wake-encounter and wake-measurement flight tests have omitted the atmospheric state data, which has a direct influence on wake flow physics. The NASA Langley Research Center conducted a series of flight tests from 1995 through 1997 to develop a wake encounter and wake-measurement data set with the accompanying atmospheric state information. The wake vortex flight tests involved three NASA airplanes as illustrated in Figure 2.

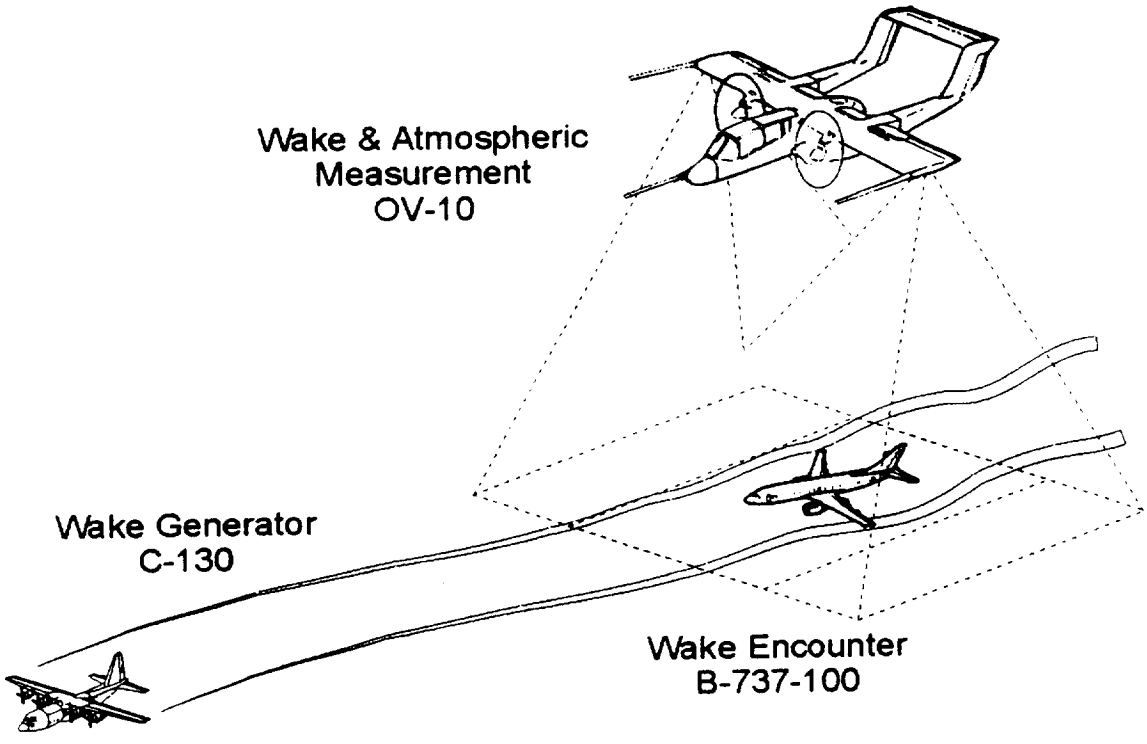

Figure 2: Wake encounter flight test setup.

The NASA Wallops Flight Facility's C-130, shown in Figure 2 and in Figure 3, was the wake generator. It was outfitted with wing tip smokers to mark the wake. It weighed between 105,000 and 95,000 pounds during the test and has a wing span of 132 feet 7 inches [19]. The NASA Langley B-737, depicted in Figure 3, flew both dynamic and steady wake encounter maneuvers through the vortex wake. Each flight contained 30-45 wake encounters, or "runs", which varied from 4-7 seconds in length. During these runs, the control surface positions as well as forces and moments were recorded onboard the B-737 in 0.05 second increments. The B-737 was approximately the same weight as the C-130. A photograph of a vortex encounter, taken from a camera mounted on top of the B-737 vertical tail, is shown in figure 4.

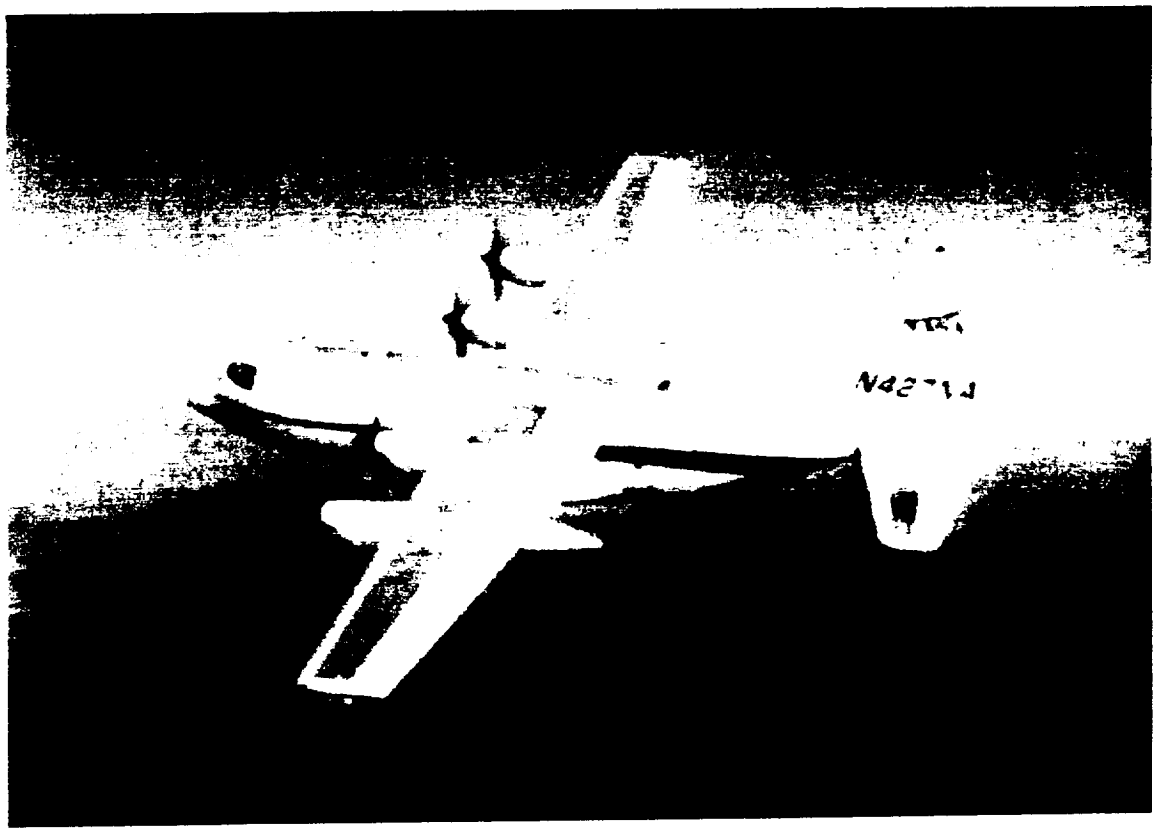

Figure 3: C-130 wake generator airplane.

The wake position relative to the B-737 was recorded using an experimental wing-mounted stereoscopic video system on-board a specially instrumented OV-10A airplane, shown in figure 5. The OV-10 flew above the B-737 to video record the wake encounter, as illustrated in figure 6. Figure 4 shows a picture taken with this video system of the B-737 encountering a wake. The position of the vortices relative to the B-737 was computed post-flight from the stereoscopic shift of the images between the left and right wing tip cameras.

Figure 4: Tail video of B-737 wake encounter.

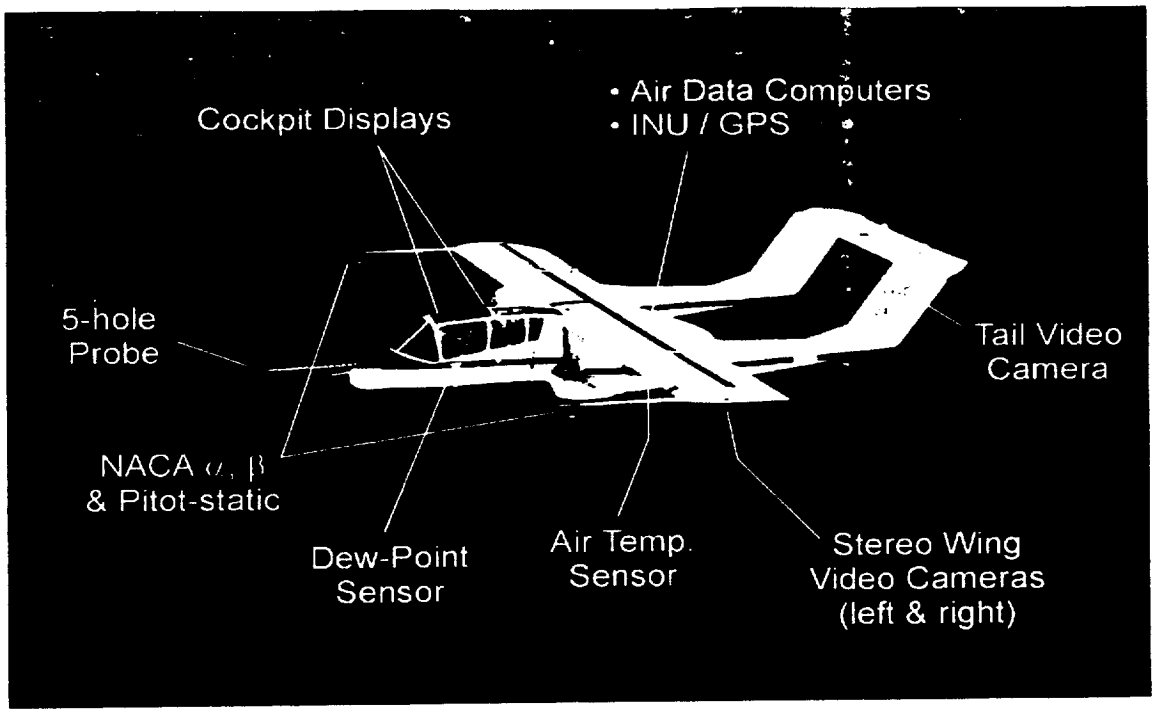

Figure 5: OV-10 major instrumentation systems

The OV-10 was also used to measure the flow field characteristics of the wake using a three-boom, flow-sensor arrangement on the aircraft. After the B-737 completed a series of wake encounter maneuvers at a fixed distance from the C-130, the OV-10 would descend and fly through the wake, measuring its velocities and position. The OV-10 was also equipped to measure the ambient weather conditions for correlation with the wake transport and decay characteristics.

Figure 6: OV-10 left wing video image of B-737 wake encounter.

This study analyses NASA LaRC's flight tests data collected from 1995 to 1997. The primary focus of this research is to establish a procedure for computing the wake-induced forces and moments imparted on the B737 using the flight measurements recorded during those earlier flights. This computed data will serve as the foundation for a comprehensive wake database, including the corresponding atmospheric state data. Fellow researchers will then use the wake database for comparison and validation of current and future simulations. The information gained from this research, and others that follow, is vital to the FAA's efforts of establishing new separation guidelines during instrument flight rules.

CHAPTER 2: METHODOLOGY

2.1 Approach

As stated previously, NASA Langley Research Center conducted a series of flight tests from 1995-1997 with the express purpose of developing a comprehensive database consisting of wake-vortex measurements and wake-vortex/aircraft interaction data, along with the accompanying atmospheric conditions. This database would then be used for comparison and validation of experimental and computational simulations and their results. Using data from those flights, this research focused on describing the wake-vortex/ aircraft interaction by computing the wake-induced forces and moments imparted on the B737-100 aircraft.

To derive the wake-induced forces and moments (FAM_{wi}) imparted on the B737, it was necessary to use the motion and control deflection variables recorded onboard the aircraft (AC). This flight data was initially put into a modified B737 simulation, whereby the FAM of the AC out of the wake's presence ($FAM_{no\ wake}$) were computed. Using the same flight data, the aircraft's forces and moments in the wake's presence (FAM_{wake}) were derived by employing a series of transformation and motion equations. The difference on the two sets of FAM yielded the wake-induced forces and moments.

$$FAM_{wi} = FAM_{wake} - FAM_{no\ wake} \qquad 2.1.1$$

2.2 Modified Simulation

In order to compute the forces and moments (FAM) of the B737 out of the presence of the wake, it was necessary to create a modified six degree-of-freedom real-life simulation of NASA Langley's Advanced Transport Operating System (ATOS) B737-100 research aircraft. The original simulation was created for the purpose of studying the major systems onboard the aircraft (engine, landing gear, pitch control, roll control, yaw control, etc.) in addition to computing the aircraft's FAM. For the purpose of this research, it was necessary to modify this simulation by isolating the FAM subroutine and determining which control state variables were required for its operation.

Validation of the modified simulation, called Wv27b, was accomplished in a two step process. The first step consisted of inputting a test case into the original simulation.

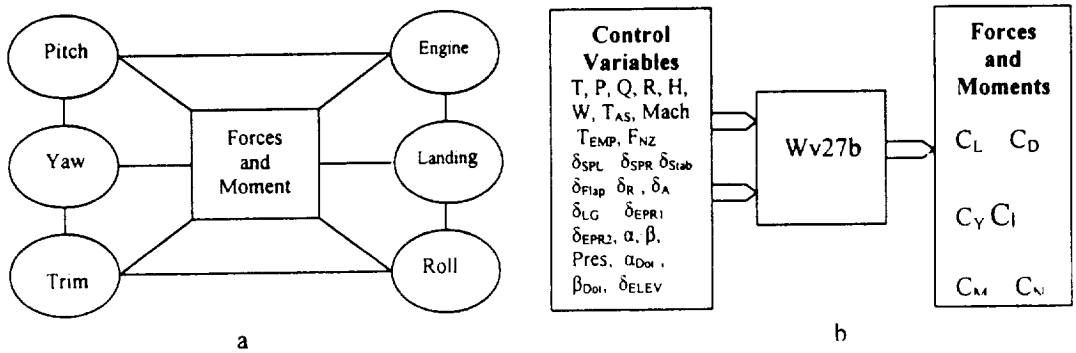

Figure 7: a. Original Simulation; b. Modified Simulation

This original simulation then created data files containing both the aircraft's FAM and the control state variables required for the modified simulation. The data file containing the control variables was then input into Wv27b whereby a second set of forces and moments were derived. The modified simulation was considered valid when the two sets of FAM were considered equal.

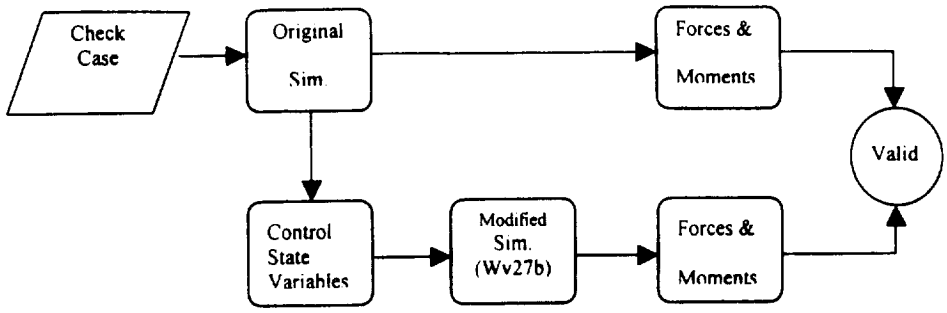

Figure 8: Modified Simulation Validation Schematic

The final procedure in computing the FAM of the B737 aircraft out of the wake's presence consisted of mapping the control state variables to the flight data variables. Using the actual flight data it was then possible to compute the forces, moments, engine thrust values, and moments of inertia of the Boeing 737-100 aircraft.

2.3 Angle of Attack and Sideslip Angle

During the Wv27b simulation validation process, it was observed that the wind speeds and directions recorded onboard the B737 were inaccurate at high bank angles. This was due to the onboard sensors adding the aircraft's weight into the wind speed and direction readings. These readings led to faulty attack and sideslip angle calculations. Ultimately, a decision was made to calculate the average wind speed and direction when the bank angle ranged between 2 and –2 degrees. These values were then used to calculate the attack and sideslip angles.

The first step in determining the attack and sideslip angles was to compute the wind and aircraft velocity components. This consisted of solving for the north (W_N), east (W_E), and vertical (W_Z) wind components in terms of the inertial, or Earth, axis system:

$$W_N = -1.688 * V_{WND} * \cos(\Psi_{WND}) \qquad 2.3.1$$

$$W_E = -1.688 * V_{WND} * \sin(\Psi_{WND}) \qquad 2.3.2$$

$$W_Z = 0 \text{ (assumed negligible)} \qquad 2.3.3$$

Since the east (V_E), north (V_N), and vertical (V_Z) inertial axis velocity components were also recorded onboard the B737, it was then possible to solve for the aircraft's longitudinal (U_B), lateral (V_B), and vertical (W_B) body axis velocities:

$$\begin{pmatrix} U_B \\ V_B \\ W_B \end{pmatrix} = T^{-1}_{be} * \begin{pmatrix} V_N - W_N \\ V_E - W_E \\ V_Z - W_Z \end{pmatrix} \qquad 2.3.4$$

T^{-1}_{be} is the inverse transformation matrix used to change the values from the inertial to the body axis. This matrix is then defined using the aircraft's true heading (Ψ), pitch (θ), and bank (ϕ) angles as

$$T^{-1}_{be} = \begin{pmatrix} \cos\Psi\cos\theta & \sin\Psi\cos\theta & -\sin\theta \\ \cos\Psi\sin\theta\sin\phi - \sin\Psi\cos\phi & \sin\Psi\sin\theta\sin\phi + \cos\Psi\cos\phi & \cos\theta\sin\phi \\ \cos\Psi\sin\theta\sin\phi + \sin\Psi\cos\phi & \sin\Psi\sin\theta\sin\phi - \cos\Psi\cos\phi & \cos\theta\cos\phi \end{pmatrix} \qquad 2.3.5$$

It was then possible to solve for the angle of attack (α) and the sideslip angle (β) using the true airspeed (TAS) recorded onboard the Boeing 737-100 aircraft.

$$\alpha = \tan^{-1}(W_B / U_B) \qquad 2.3.6$$

$$\beta = \sin^{-1}(V_B / TAS) \qquad 2.3.7$$

The final procedure consisted of solving for the rates of change in the attack and sideslip angles, α_{Dot} and β_{Dot}, using three discrete approximation techniques [21]:

$$\text{Forward Approximation} = (-3*f_i + 4*f_{i+1} - f_{i+2}) / (2\Delta t) \qquad 2.3.8$$

$$\text{Backward Approximation} = (3*f_i - 4*f_{i-1} + f_{i-2}) / (2\Delta t) \qquad 2.3.9$$

$$\text{Centered Approximation} = (f_{i+1} - f_{i-1}) / (2\Delta t) \qquad 2.3.10$$

Time	α	α_{Dot}	β	β_{Dot}
Sec.	Deg.	Deg.	Deg.	Deg.
.05	6.717629	-0.35089	0.078838	0.340431
.1	6.70355	-0.21227	0.09065	0.132053
.15	6.696402	-0.23149	0.092043	0.125266
....	....	....	....	....
....	....	....	....	....
3.90	6.670654	0.022375	-0.37421	0.05243
3.95	6.667219	-0.04954	-0.37218	0.094031
4.0	6.6657	-0.01123	-0.3648	0.200809

Table 2: Rate Change of Attack and Sideslip Angles

For example, the forward approximation technique was used to solve for the initial α_{Dot} by setting α equal to "f" in eq. 2.3.8:

$$\alpha_{Dot\,(1)} = (-3*\alpha_1 + 4*\alpha_2 - \alpha_3) / (2\Delta t) \qquad 2.3.11$$

In contrast, a backward approximation was used to solve for the final α_{Dot} value:

$$\alpha_{Dot\,(n)} = (3*\alpha_n - 4*\alpha_{n-1} + \alpha_{n-2}) / (2\Delta t) \qquad 2.3.12$$

The centered approximation technique, eq. 2.3.10, was invoked for all other points in between. This procedure was then used to compute β_{Dot}.

2.4 Transformation and Motion Equations

Determining the forces and moments of the aircraft in the presence of the wake required the series of transformation and motion equations from reference 20. These force and moments were calculated within a specially designed Excel template, FLT_VS_SIM. The aircraft's body force components were derived using the weight (W), longitudinal acceleration (Acc_{Lon}), lateral acceleration (Acc_{Lat}), and normal direction acceleration (F_{NZ}) data from the B737 flight data [20]:

$$F_X = (Acc_{Lon} * W) / g \qquad 2.4.1$$

$$F_Y = (Acc_{Lat} * W) / g \qquad 2.4.2$$

$$F_Z = (F_{NZ} * W) / g \qquad 2.4.3$$

Converting these forces from the body axis to the stability axis, the lift (C_L), drag (C_D), and sideforce (C_Y) coefficients become:

$$C_L = -((F_X - T_X) \sin \alpha - F_Z \cos \alpha)/ qS \qquad 2.4.4$$

$$C_D = ((F_X - T_X) \cos \alpha + F_Z \sin \alpha)/ qS \qquad 2.4.5$$

$$C_Y = F_Y/ qS \qquad 2.4.6$$

where T_X is defined as the body axis thrust derived by the modified simulation, S is the aircraft's wing area, and q is the dynamic pressure.

The next step consisted of solving for the B737's rolling (C_l), pitching (C_m), and yawing (C_n) moments in the presence of the wake. This procedure involved computing the

total moments of the aircraft in terms of the pitch rate (Q), roll rate (P), and yaw rate (R) [20]. It was also necessary to use the B737's moments of inertia (I_{XX}, I_{YY}, I_{ZZ}, I_{XZ}) derived by Wv27b:

$$M_X = P_{DOT}*I_{XX} - R_{DOT}*I_{XZ} + Q*(R*I_{ZZ} - P*I_{XZ}) - R*(Q*I_{YY}) \quad 2.4.7$$

$$M_Y = Q_{DOT}*I_{YY} + R*(P*I_{XX} - R*I_{XZ}) - P*(R*I_{ZZ} - P*I_{XZ}) \quad 2.4.8$$

$$M_Z = R_{DOT}*I_{ZZ} - P_{DOT}*I_{XZ} + P*(Q*I_{YY}) - Q*(P*I_{XX} - R*I_{XZ}) \quad 2.4.9$$

P_{DOT}, Q_{DOT}, and R_{DOT} represented the rate changes in the roll, pitch, and yaw rates respectively. They were computed using the discrete approximations described in the previous section. Rewriting these moment equations in coefficient form gives the following three equations for the rolling moment coefficient, pitching moment coefficient, and yawing moment coefficient:

$$C_l = M_X / (qSb) \quad 2.4.10$$

$$C_m = (M_Y + T_m) / (qSc) \quad 2.4.11$$

$$C_n = (M_Z + T_n) / (qSb) \quad 2.4.12$$

T_m and T_n were added to the preceding equations to account for the thrust contributions in the pitching and yawing moments. Converting these moments to the stability axis gives,

$$C_{lS} = C_l * \cos(\alpha) + C_n * \sin(\alpha) \quad 2.4.13$$

$$C_{MS} = C_m \quad 2.4.14$$

$$C_N = - C_l * \sin(\alpha) + C_n * \cos(\alpha) \qquad 2.4.15$$

The wake-induced forces and moments exerted on the B737 aircraft are derived by modifying equation 2.1.1:

$$FAM_{wi} = FAM_{wake} - FAM_{no\ wake}$$
$$= FAM_{E.O.M} - FAM_{Wv27b} \qquad 2.4.16$$

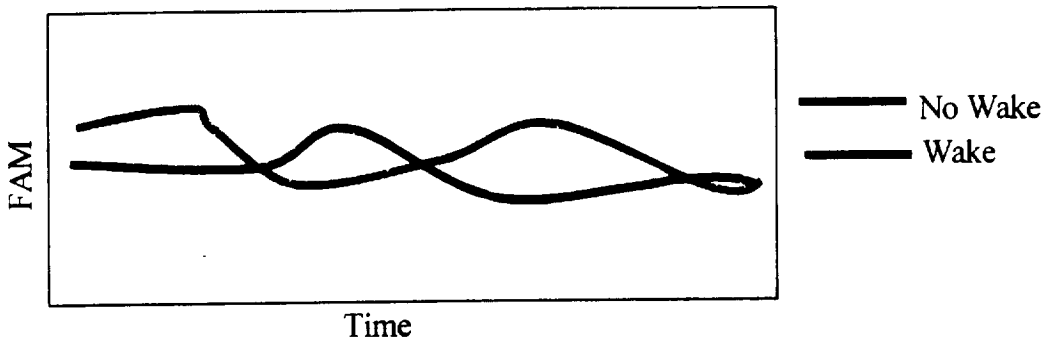

Figure 9: Example of the B737 in and out of the presence of the wake-vortex.

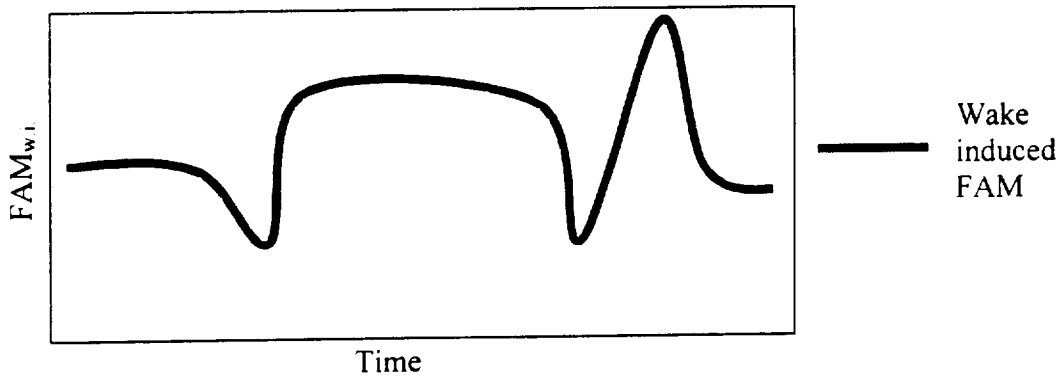

Figure 10: Example of the wake-induced forces and moments imparted on the B737.

2.5 Trim Shots

Prior to calculating the wake-induced forces and moments (FAM_{wi}), it was necessary to examine the flight data for any biases. This task was accomplished by examining the trim shots for each flight. These "trim shots" are flight segment(s) of flight in which the aircraft is placed in a trim, or level, state of flight. Trim shots were conducted before and after each flight, at flap deflections of 15 and 30 degrees.

To determine the data bias in a particular flight, the trim shot data at a flap deflection of 15 degrees was input into the Wv27b simulation and the equations of motion. This action produced two sets of forces and moments (FAM). The differences in the two sets of FAM yielded the flight data bias at that flap setting:

$$FAM_{bias} = FAM_{E.O.M} - FAM_{Wv27b} \qquad 2.5.1$$

This process was repeated using the trim shot data at a flap deflection of 30 degrees. Both sets of FAM_{bias} were then averaged to determine the mean flight data biases ($FAM_{M\,bias}$) for the entire flight. This procedure was performed for each flight.

Flight No.		C_L M. bias	C_D M. bias	C_Y M. bias	$C_{l\,s}$ M. bias	C_{MS} M. bias	C_N M. bias
558		.008016	.003821	.002287	-.015421	-.000031	-.001344
559		.042408	.014145	.012470	.012136	.003703	.000910
560		.018742	.002224	.007097	-.019048	.001341	.003738
561		.064694	-.000504	-.000203	.004717	-.000547	-.000389

Table 3: Mean flight data biases

Once the mean flight data biases were computed, the wake-induced forces and moments of each "event", or wake encounter, in a flight was calculated by modifying equation 2.1.1:

$$FAM_{wi} = FAM_{wake} - FAM_{no\ wake} - FAM_{M.bias} \qquad 2.5.2$$

It was also necessary to determine the "age" of the wake-vortex during each event. This age was defined as the time between the creation of the wake and its interception by the B737. The wake's age was computed by using the wake velocity program (Wake_Vel) described in reference [19]. As a result, the average FAM_{wi} for each event were plotted as a function of the wake's age. The final step consisted of adding error bars to denote the minimum and maximum values of the average FAM_{wi}.

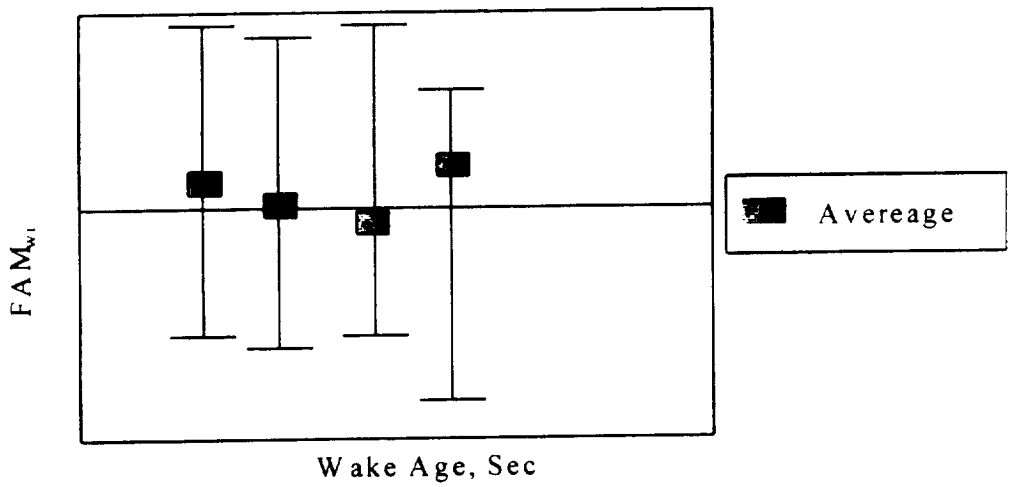

Figure11: Average forces and moment value as a function of wake age.

CHAPTER 3: RESULTS

Previously, methods of calculating the forces and moments (FAM) of an aircraft both in and out of a wake's presence were introduced. These techniques made it possible to derive the wake-induced forces and moments (FAM_{wi}) imparted on the Boeing 737 flown in NASA LaRC's flight tests. During each of these flights, flap deflection alternated between 15 and 30 degrees while separation distances ranged from 1-3 nautical miles. In addition, the B737 encountered the wake vortex using a variety of flight maneuvers, described in more detail in Section 3.3. The purpose of this research was to analyze the wake-induced forces and moments contained in each flight based on three criteria: flap deflection, separation distance, and flight maneuver.

3.1 Flap Deflection

The first analysis performed in this research looked at the effects of flap deflection on the wake-induced forces and moments. This study was conducted using the event, or wake encounter, data from each flight to generate the wake-induced forces and moments (FAM_{wi}). The chart below lists the separation distance of each flight considered in the current study:

FLIGHT	Separation Distance
558	2
559	1
560	2
561	2

Table 4: Separation distances, in nautical miles.

Looking at the wake-induced lift coefficient (C_{Lwi}) in Figures 13 and 14, there appears to be a clear difference in the average value in flights 558 and 559. At flap deflection of 15 degrees, the average C_{Lwi} was slightly higher. However, this pattern was not repeated in flights 560 or 561. In these flights, there was no clear distinction between 15 and 30 degrees. Similar results were demonstrated in the wake-induced drag coefficient (C_{Dwi}), Figures 15 and 16. In flights 558 and 559, C_{Dwi} was greater at flaps 30. The contrary was true for flights 560 and 561. This was also the case for the wake-induced pitching moment (C_{Mwi}), Figures 21 and 22.

Analysis of the sideforce (C_{Ywi}), rolling moment ($C_{l\,Swi}$), and yawing moment (C_{Nwi}) yielded results which were more definite. In each flight, the averages of the forces and moments were constant for flap settings of 15 and 30. However, the values of the average FAM were not the same for each flight.

In conclusion, analysis of the wake-induced forces and moments based on flap separation suggested that there was no difference in the wake effect at the two different flap settings. This is reflected in the average values of C_{Ywi}, $C_{l\,Swi}$, and C_{Nwi}. The wake-induced lift, drag, and pitching moment seemed to support this outcome also in flights 560-61.

3.2 Separation Distance

The second criterion analyzed in this research was that of separation distance variation. The purpose of this analysis was to determine if reducing separation distances increased the effects of the wake. This study was conducted using the encounter data from flight 558,559,and 560 to generate the wake-induced forces and moments (FAM_{wi}). The separation distances in these encounters ranged from 1-3 nautical miles while flap deflection was constant at 30 degrees. Flight 561 was omitted from this analysis due to insufficient amounts of data at 3nm.

Upon analyzing the data, it was apparent that variations in these separation distances had no profound impact on some of the wake-induced forces and moments. In Figure 25, the average wake-induced lift coefficient (C_{Lwi}) was consistent between 1nm and 2nm, ranging from –0.1 to 0.1. Similar findings were demonstrated between 2nm and 3nm in flight 560. This pattern was mimicked in the wake-induced sideforce (C_{Ywi}) and yawing moment (C_{Nwi}), in Figures 27 and 30 respectively. For the case of the wake-induced drag coefficient (C_{Dwi}), Figure 26, it was noticed that the average was consistent at 1-2nm; yet, the average C_{Dwi} was slightly less at 3nm. This supports the hypothesis of wake-induced drag reducing as the separation distance increases.

Analysis of the FAM_{wi} provided inconclusive results in the areas of pitching and rolling moment. Looking at the wake-induced pitching moment (C_{Mwi}) in flights 558 and 560, the average initially appeared to increase slightly as the separation distance increased, as shown in Figure 29. In contrast, the average in flight 559 suggested that the average between 1-2nm was roughly equal, thus making the results from the other flights inconclusive. The same situation occurred in evaluation of the wake-induced rolling moment ($C_{l\,Swi}$). These results are depicted in Figures 28.

In conclusion, data reflected there no significant difference in the wake-induced lift, drag, sideforce, or yawing moment between 1-3nm. In the cases of the wake-induced pitching and rolling moment, the results were inconclusive. Preliminary results indicate that both increase as the separation distance increases; however, more flight data is required before a definitive conclusion may be reached.

3.3 Maneuver Comparison

In NASA LaRC's flight tests, the Boeing 737 executed a series of flight maneuvers, or patterns, as it penetrated the wake vortex. These patterns were defined as out-to-in (OTI), in-to-out (ITO), down-to-up (DTU), and up-to-down (UTD).

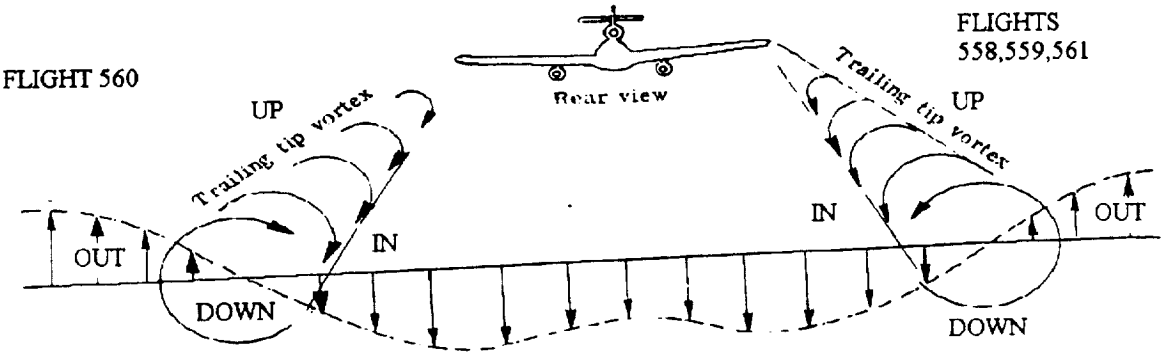

Figure 12: Description of flight maneuvers

The purpose was to determine the affects of the wake-induced forces and moments (FAM_{wi}) on the aircraft during these penetrations. To perform this analysis, the FAM_{wi} originated from wake encounter data taken in each flight. In these flights, the separation distance and flap deflection remained constant, allowing only the flight maneuver to change.

Flight #	Flap Deflection	Separation Distance
558	15	2nm
559	30	1nm
560	15	2nm
561	15	2nm

Table 5: Flap deflection and separation distance constants

Analysis of the wake-induced forces and moments of varying flight patterns did provide some useful information. Looking at the wake –induced lift coefficient (C_{Lwi}) in Figures 31 and 32, OTI maneuvers appear to have the largest average values in every flight. This suggests that the wake imposed more lift on the aircraft in this situation than in any other. In contrast, ITO exhibits some of the lowest averages. This is probably due to both vortices initially acting on an aircraft during this flight maneuver. OTI and ITO also seemed to display the highest degrees of disparity throughout the four flights. This translates into a large degree of upset, or turbulence, for the aircraft. Similar results were also found true for wake-induced pitching (C_{Mwi}) and rolling moments ($C_{l\,Swi}$), shown in Figures 39 -40 and Figures 37-38 respectively.

Focusing attention on the affects of the wake-induced drag coefficient (C_{Dwi}), results for OTI and DTU maneuvers show the lowest average values for all flights. These values usually ranged around .01, Figures 33 and 34. As for the wake-induced sideforce coefficient, DTU maneuvers display the highest degree of fluctuation between minimum and maximum average for Flights 558-560. This data suggests that the aircraft experienced a noticeable sideforce, or crosswind force, when it traversed the wake from

up to down. The reverse is true for Flight 561, where the crosswind force was noticed when the B737 penetrated the wake in a down to up motion.

For cases involving the wake-induced yawing moment (C_{Nwi}), the results were rather inconclusive. No consistent pattern of consistency was exhibited in the average C_{Nwi} for any of the maneuvers. This pattern was repeated in each of the flights, Figures 35 and 36.

In conclusion, the wake appeared to influence the aircraft in each of the flight maneuvers. Generally, these effects were felt most during out-to-in and in-to-out maneuvers. This is evident in cases involving wake-induced lift, drag, sideforce, rolling moment, and pitching moment. In contrast, the results were inconclusive for the wake-induced yawing moment. For this reason, more flight data has to be generated before a definitive conclusion can be obtained.

CHAPTER 4: CONCLUSION

Airports are becoming capacity limited. In order to alleviate this situation, it is necessary to increase the number of operations per runway during Instrument Flight Rules (IFR) by decreasing current separation distances. In response to this demand, the NASA Langley Research Center conducted a series of flight tests from 1995 through 1997 to develop a wake encounter and wake-measurement data set with the accompanying atmospheric state information. The purpose of the research presented here was to design and implement a procedure to calculate the wake encounter portion of that database using the flight data from those earlier flight tests. The results from this study will be stored in a comprehensive database that will be available to the FAA for use in evaluating reduced separation guidelines. This database will also be used by other researchers for comparison and/or validation of current and future encounter simulations.

In order to calculated the wake-induced forces and moments imparted on the Boeing 737, it was necessary to devise separate methods of calculating the aircraft's forces and moments in and out of the presence of the wake vortex. Initially, this research created a simulation to calculate the FAM of the B737 out of the presence of the wake- vortex using the data recorded during NASA's flight tests. This simulation, called Wv27b, was formed using a real-life simulation of NASA Langley's Advanced Transport Operations System (ATOS) research airplane. The next step of consisted of using the flight data in a series of fundamental transformation and motion equations to calculate the aircraft's FAM while in

the presence of the wake-vortex. Finally, the difference in the two sets of calculated forces and moments resulted in the wake-induced forces and moments ($FAM_{w,i}$).

There were three objectives of this research. Initially, the wake-induced forces and moments ($FAM_{w,i}$) from each flight were analyzed based on varying flap deflection angles. The flap setting alternated between 15 and 30 degrees while the separation distance remained constant. This examination was performed in order to determine if increases in flap deflection would increase or decrease the effects of the wake-induced forces and moments. Next, the wake-induced forces and moments from each flight were analyzed based on separation distances of 1-3 nautical miles. In this case, flap deflection was held constant at 30 degrees. The purpose of this study was to determine the degree to which reducing separation distances increased the effects of the wake vortex on the aircraft. The last objective was accomplished by comparing the $FAM_{w,i}$ of each flight as it executed a series of maneuvers, or patterns, through the wake-vortex. This analysis was conducted to determine if one maneuver was more susceptible than another in a wake's presence. To perform this comparison, the separation distance and flap setting were held constant for each flight.

Results from the first analysis indicated that there was no difference in wake effect at flap deflections of 15 and 30 degrees. This conclusion is evidenced in the cases of C_{Ywi}, C_{LSwi}, and C_{Nwi}. The wake–induced lift, drag, and pitching moment cases yielded less conclusive results. The second analysis compared the wake-induced forces and moments at separation distances of 1-3 nautical miles. Results indicated that there was no significant difference in the wake-induced lift, drag, sideforce, or yawing moment coefficients. The last analysis compared the wake-induced forces and moments based on different flight maneuvers. It was found that the FAM_{wi} had the greatest impact on OTI and ITO maneuvers.

Plans to further this research involve a comparative analysis of these results to those obtained by Pete [25]. Her research sought to validate the strip theory and vortice lattice modeling techniques. The forces and moments of both models with their full geometry (wings, horizontal stabilizer, vertical stabilizer) were compared to the data from an experimental model. Comparisons were also performed using the partial geometry (horizontal and/or vertical stabilizer removed) of the three models to determine if the models still had an acceptable accuracy. Pete also performed a sensitivity analysis to observe the accuracy of the models if there was a 10% error in the models' input data. Another comparison which to be conducted in the future will consist of using the results from a wind tunnel experiment conducted by NASA. In this case, a pilot flew a 10% scale of a B737 aircraft inside a wind tunnel. The scale model was flown at different locations with respect to the vortex whereby the forces and moment s of the encounter were recorded.

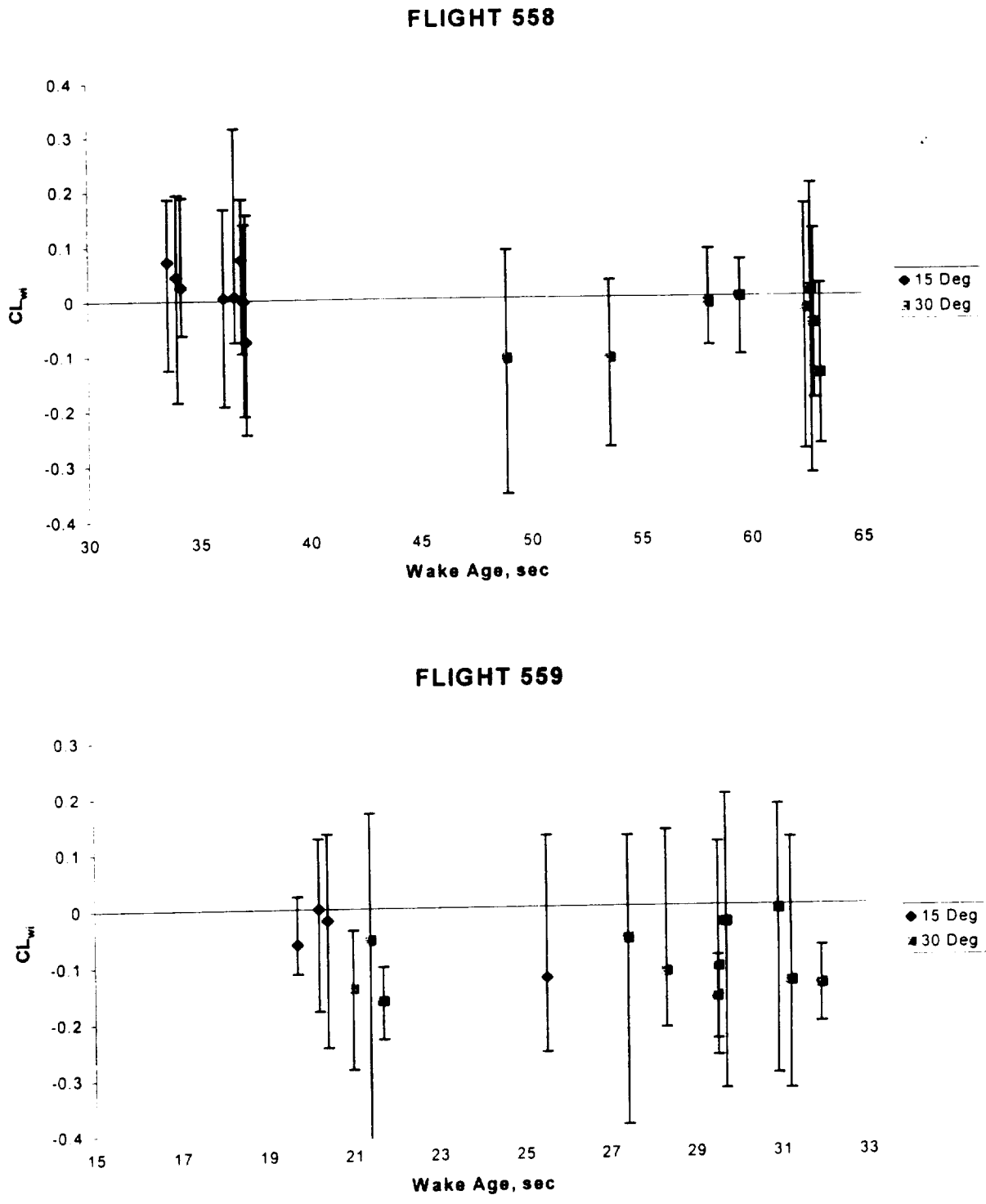

Figure 13: Wake-induced lift coefficient, based on flap deflection.

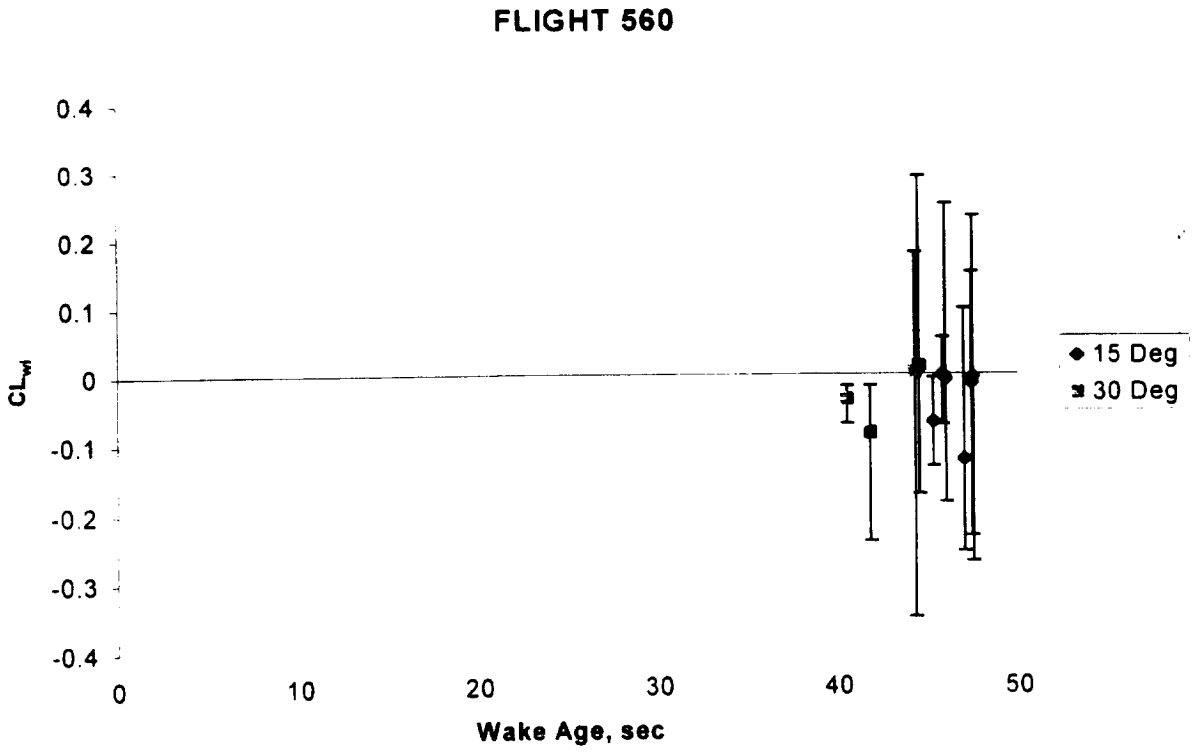

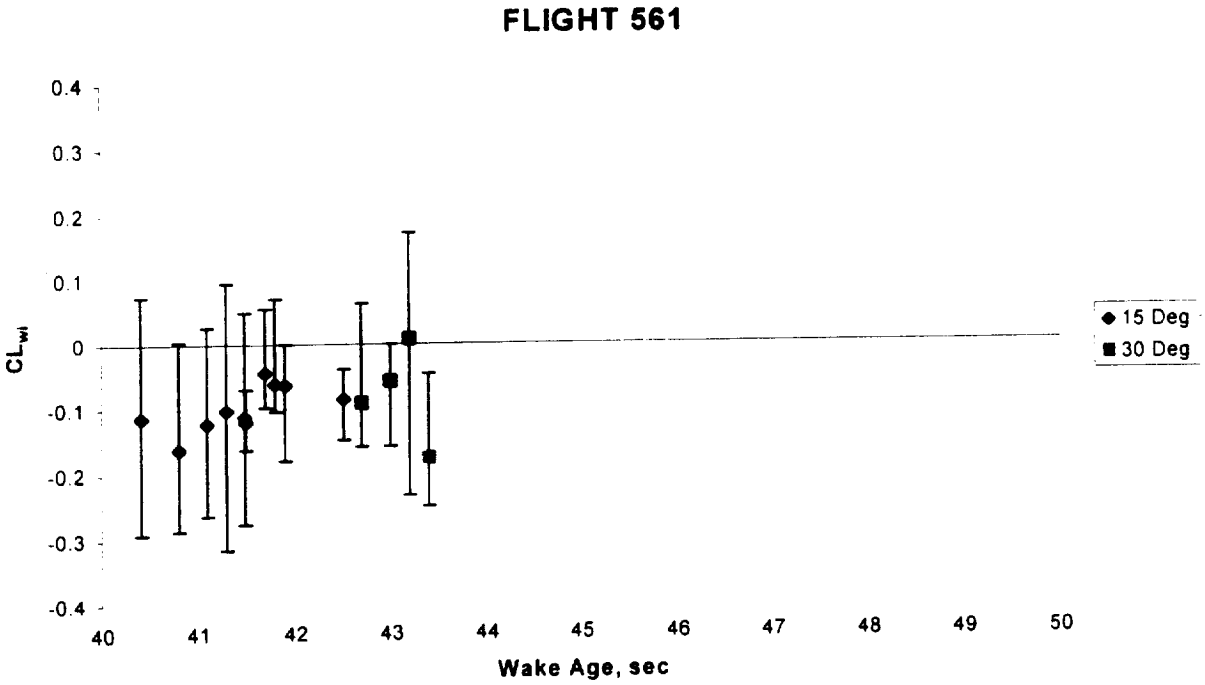

Figure 14: Wake-induced lift coefficient , based on flap deflection.

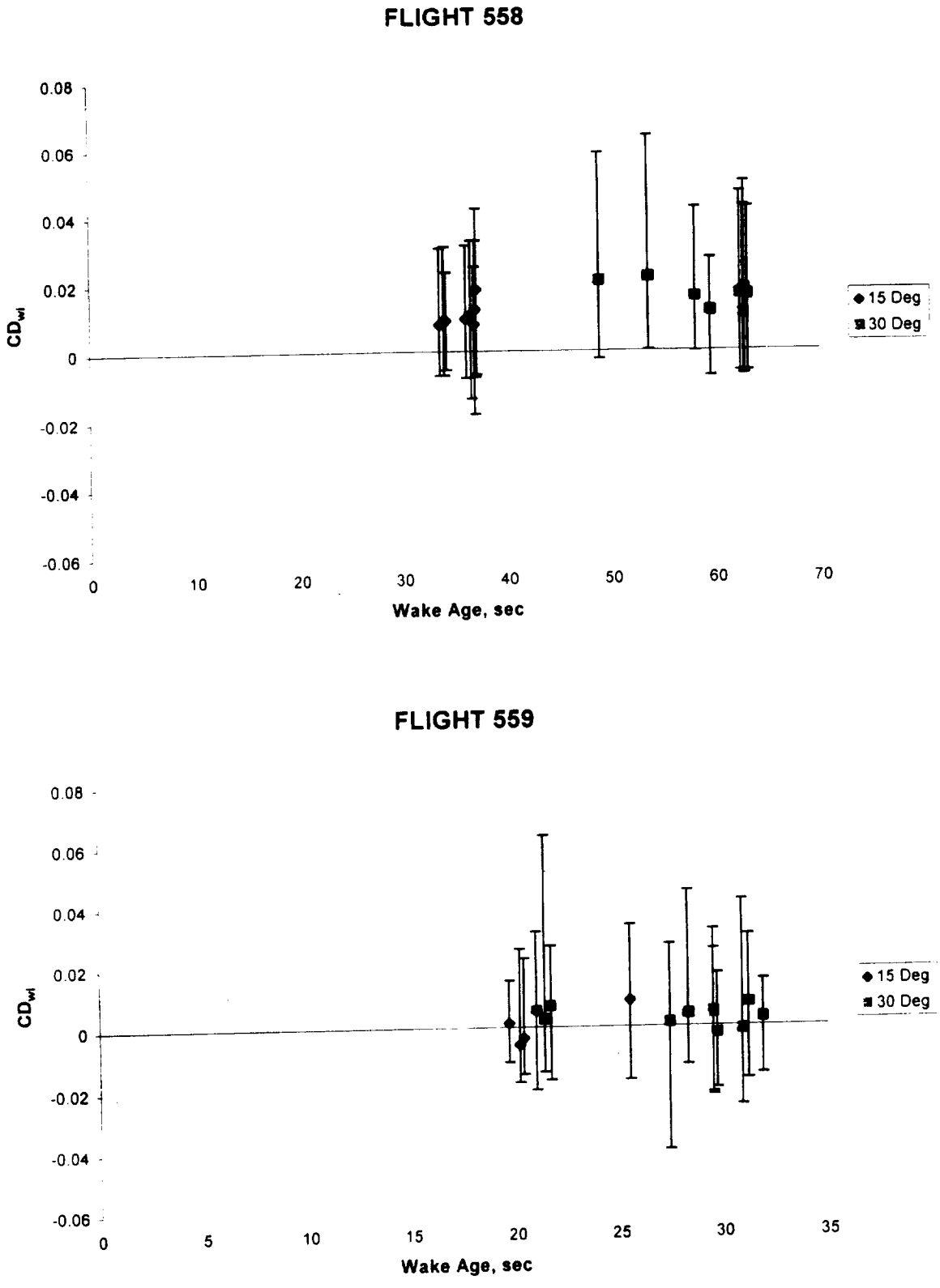

Figure 15: Wake-induced drag coefficient, based on flap deflection.

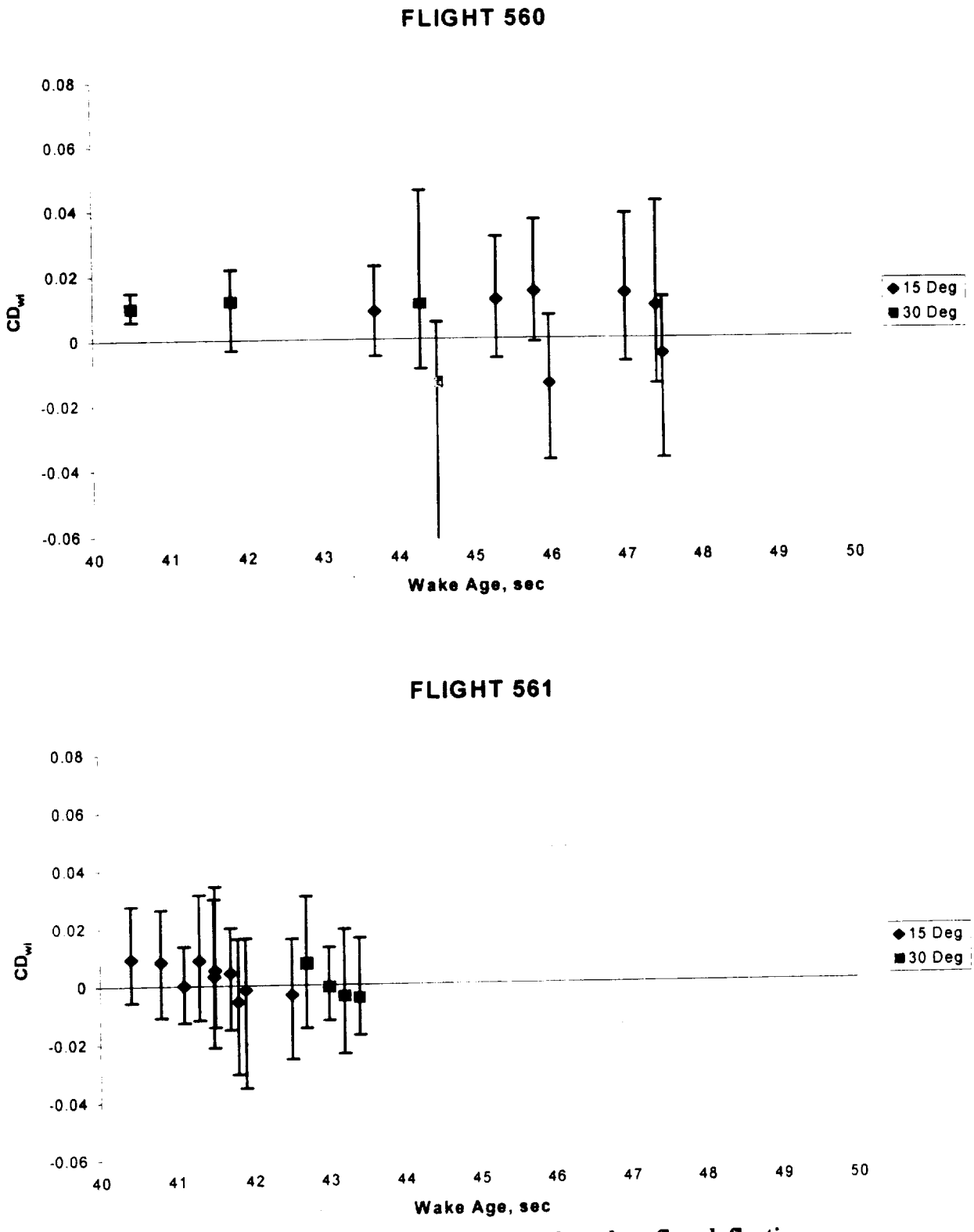

Figure 16: Wake-induced drag coefficient, based on flap deflection.

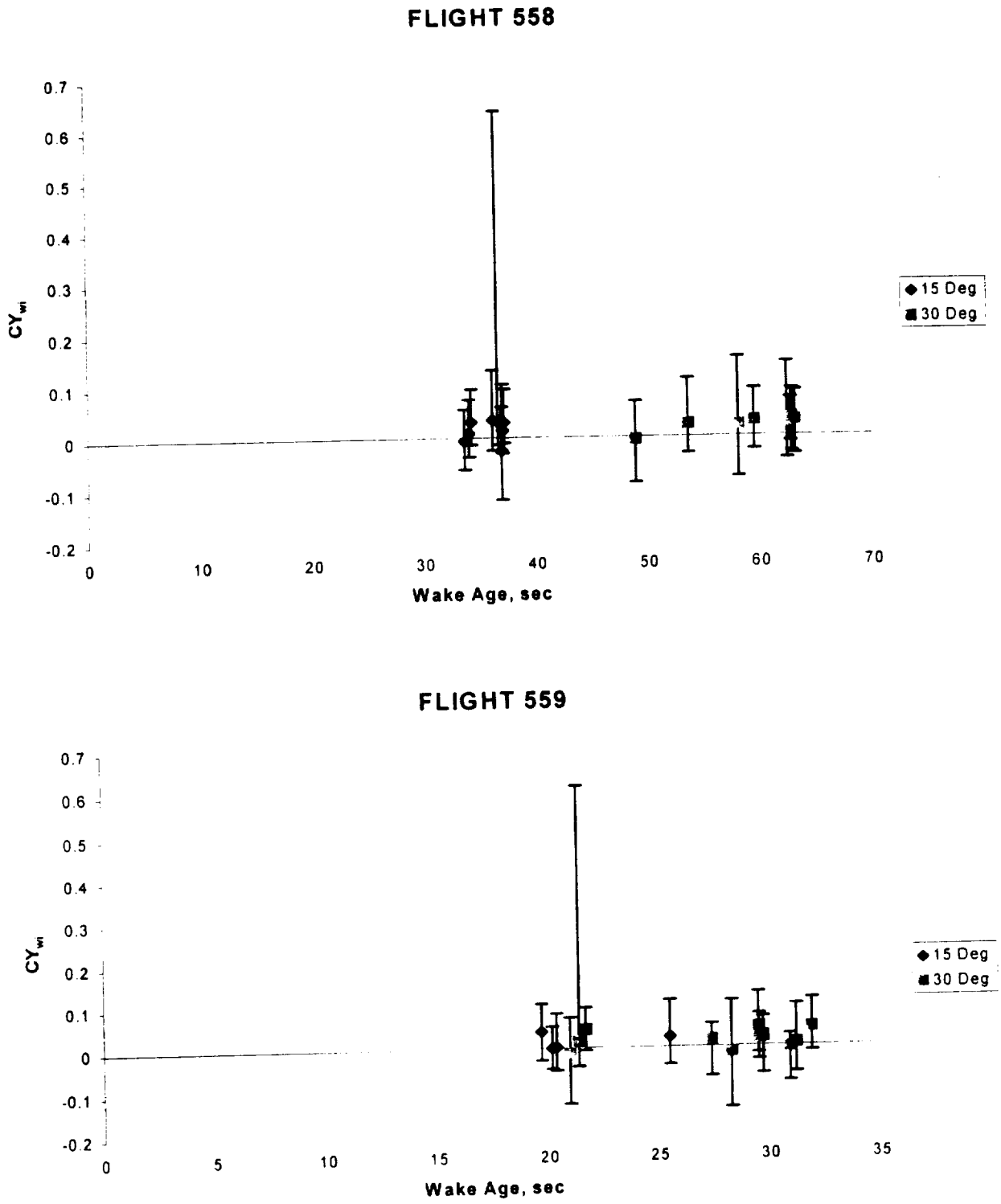

Figure 17: Wake-induced sideforce coefficient, based on flap deflection.

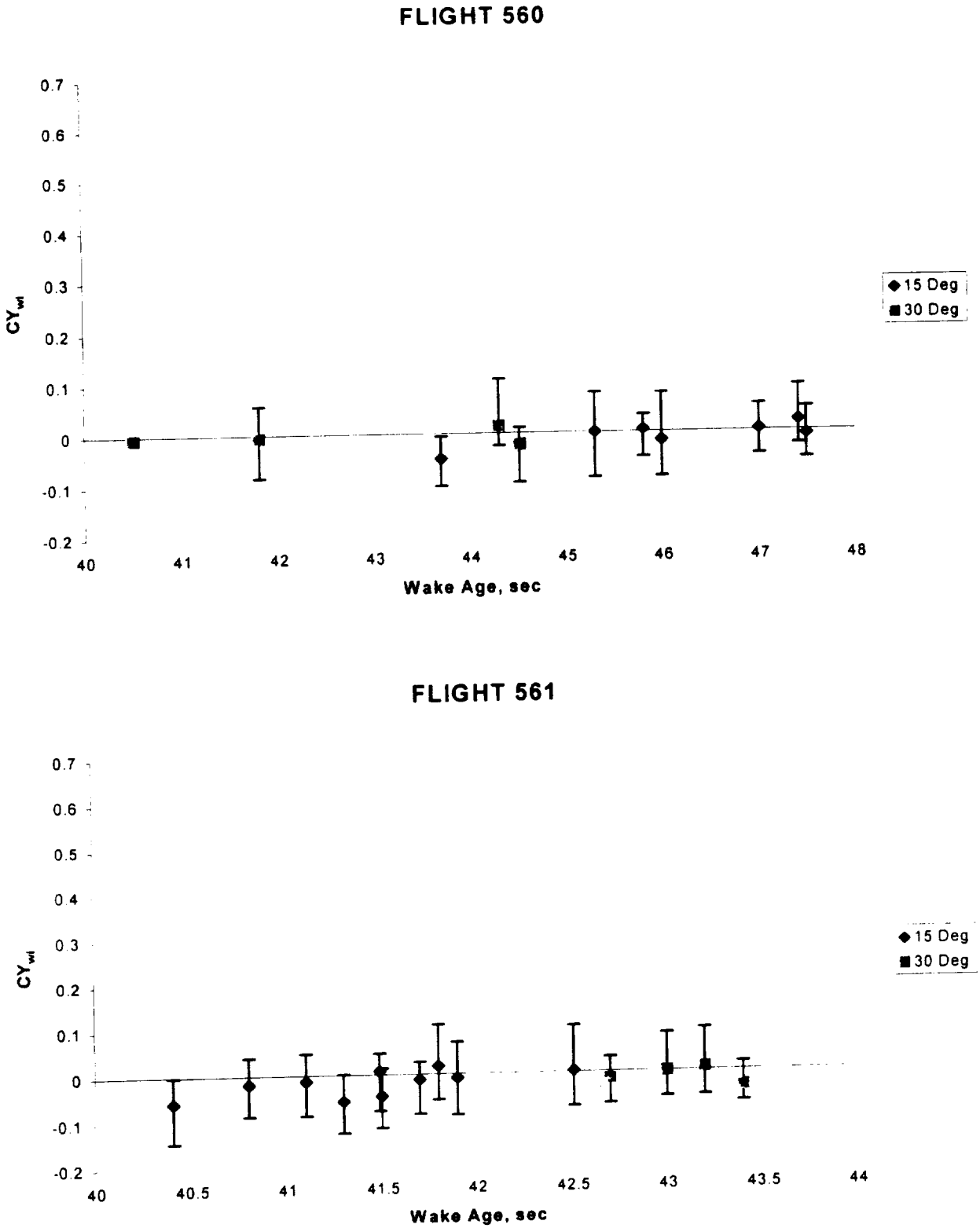

Figure 18: Wake-induced sideforce coefficient, based on flap deflection.

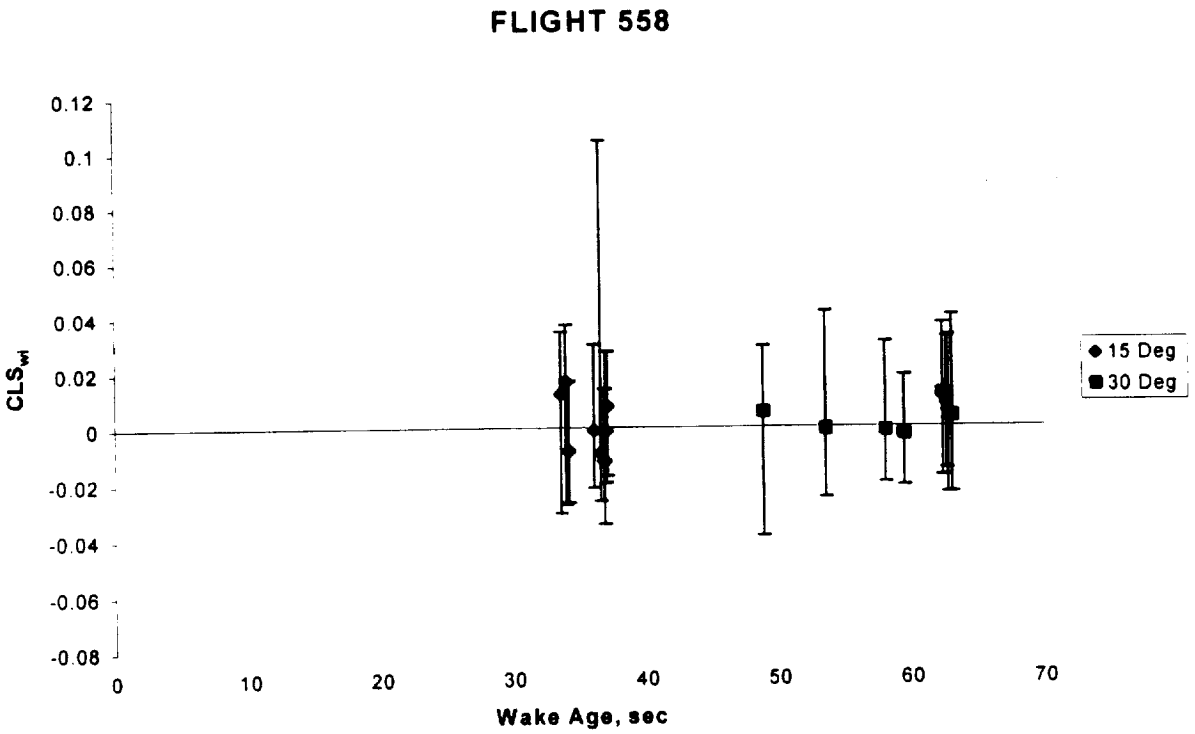

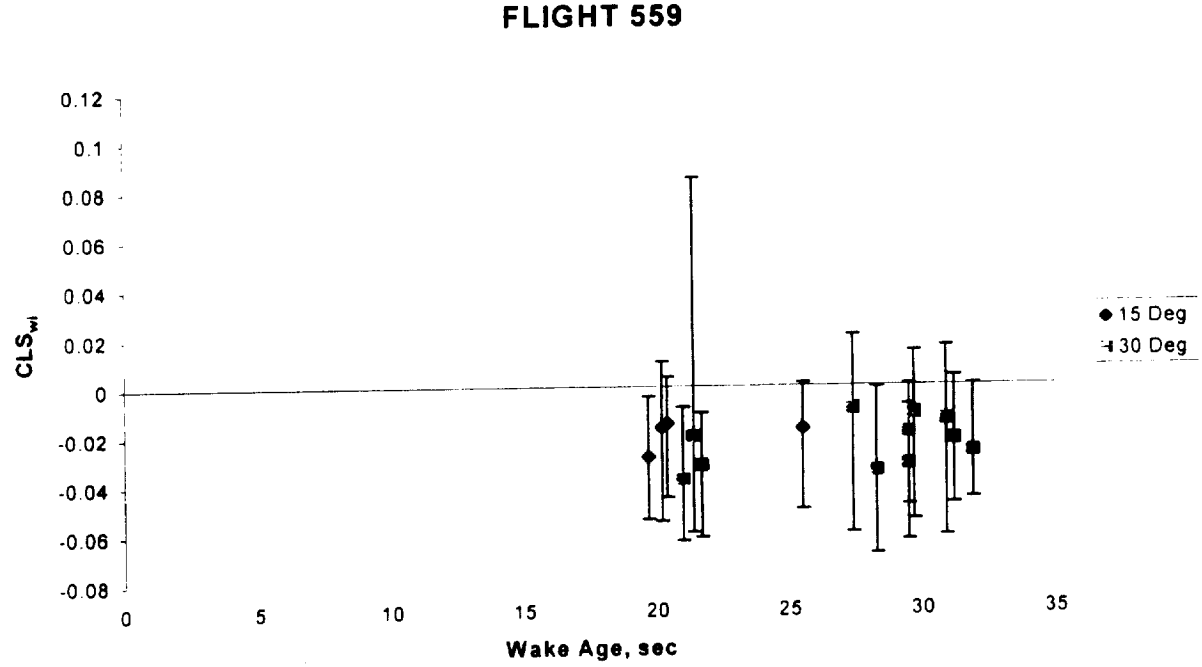

Figure 19: Wake-induced rolling moment coefficient, based on flap deflection.

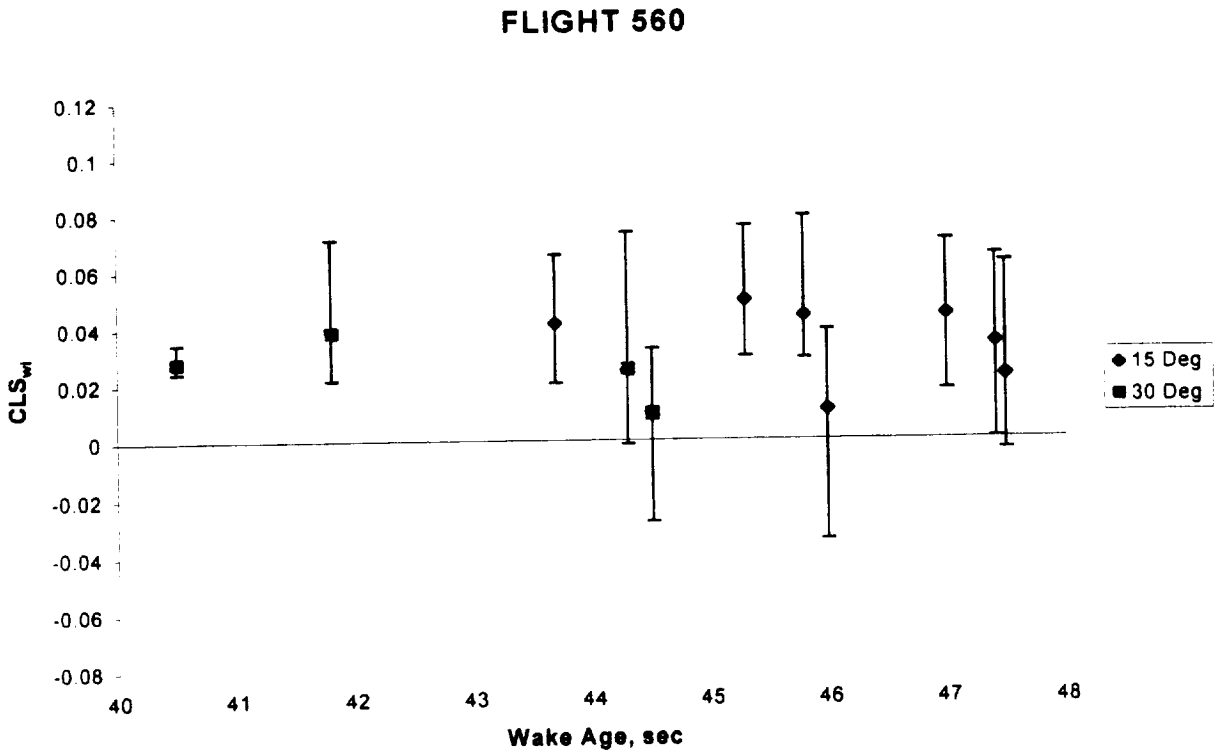

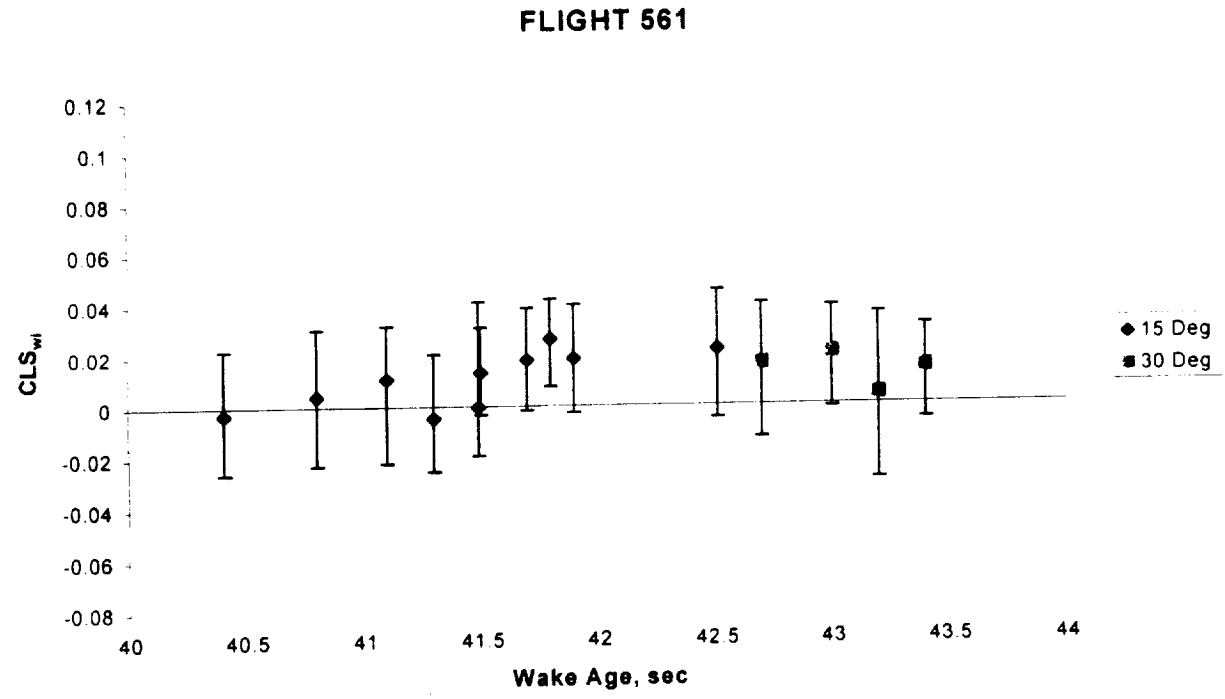

Figure 20: Wake-induced rolling moment coefficient, based on flap deflection.

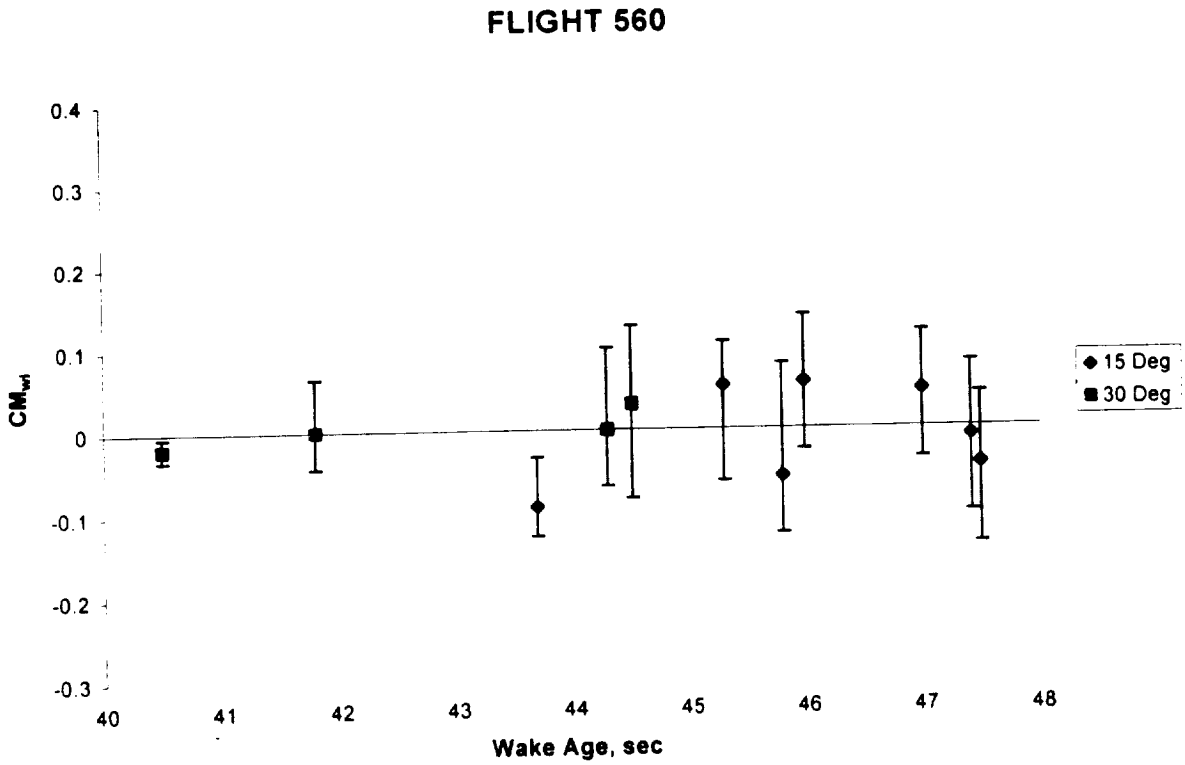

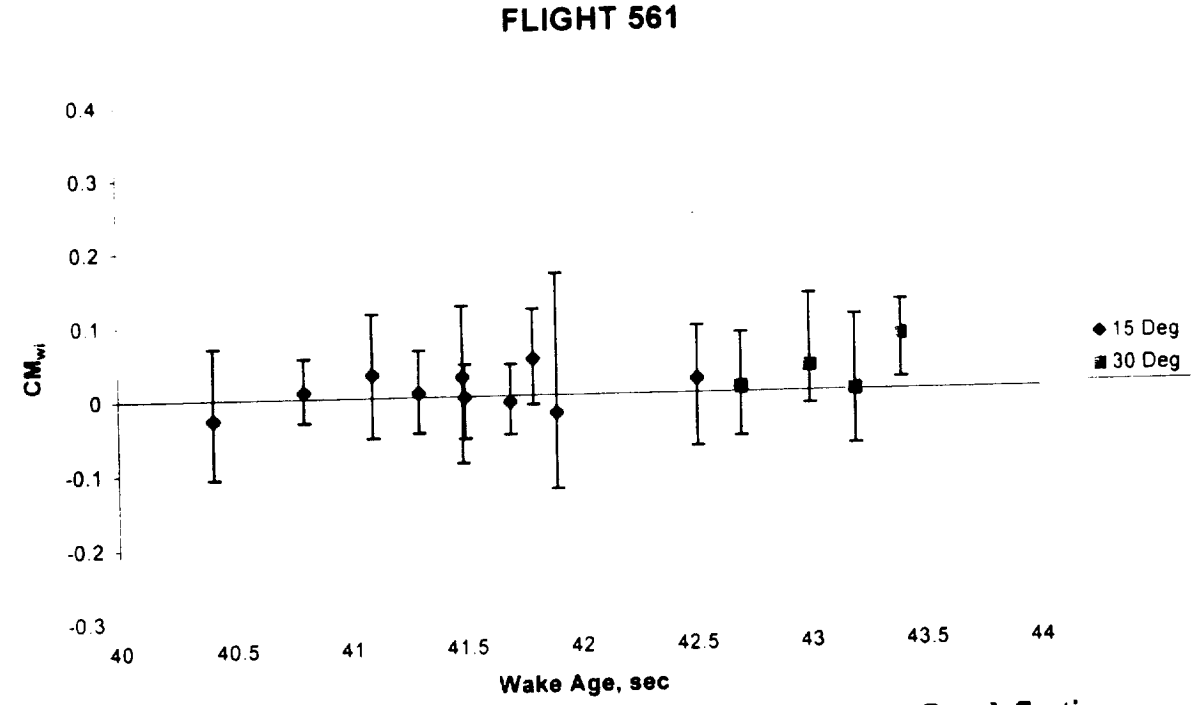

Figure 21: Wake-induced pitching moment coefficient, based on flap deflection.

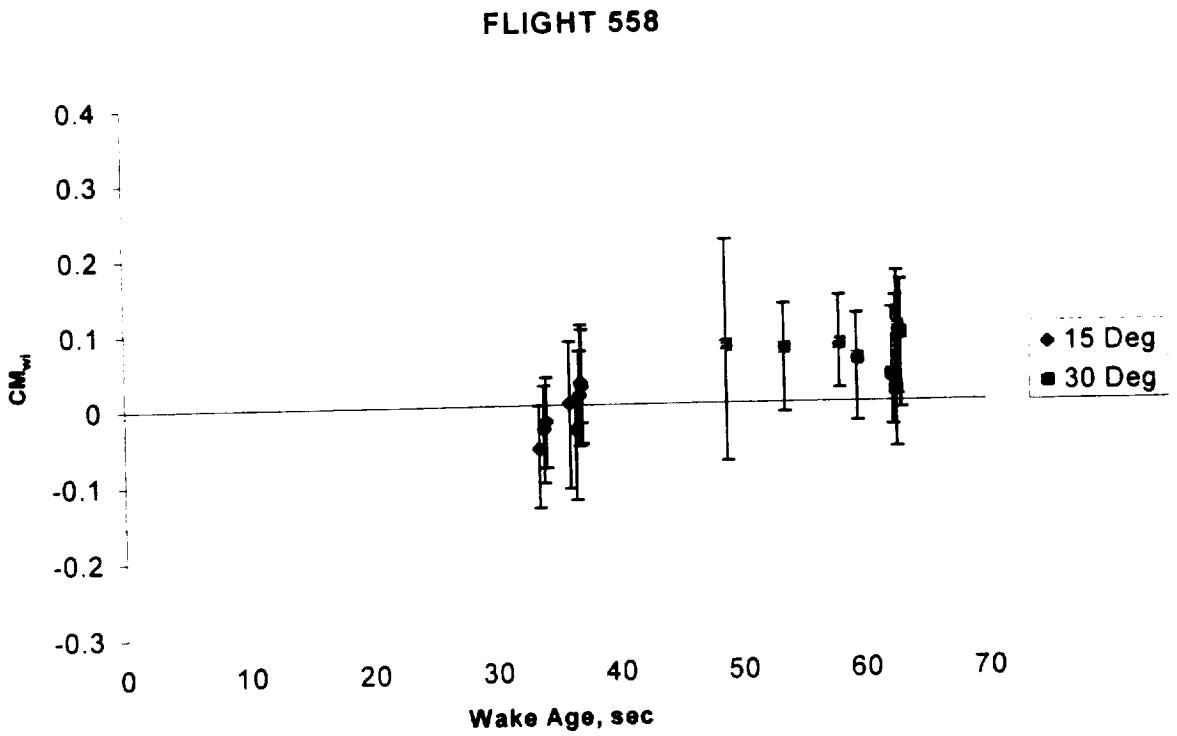

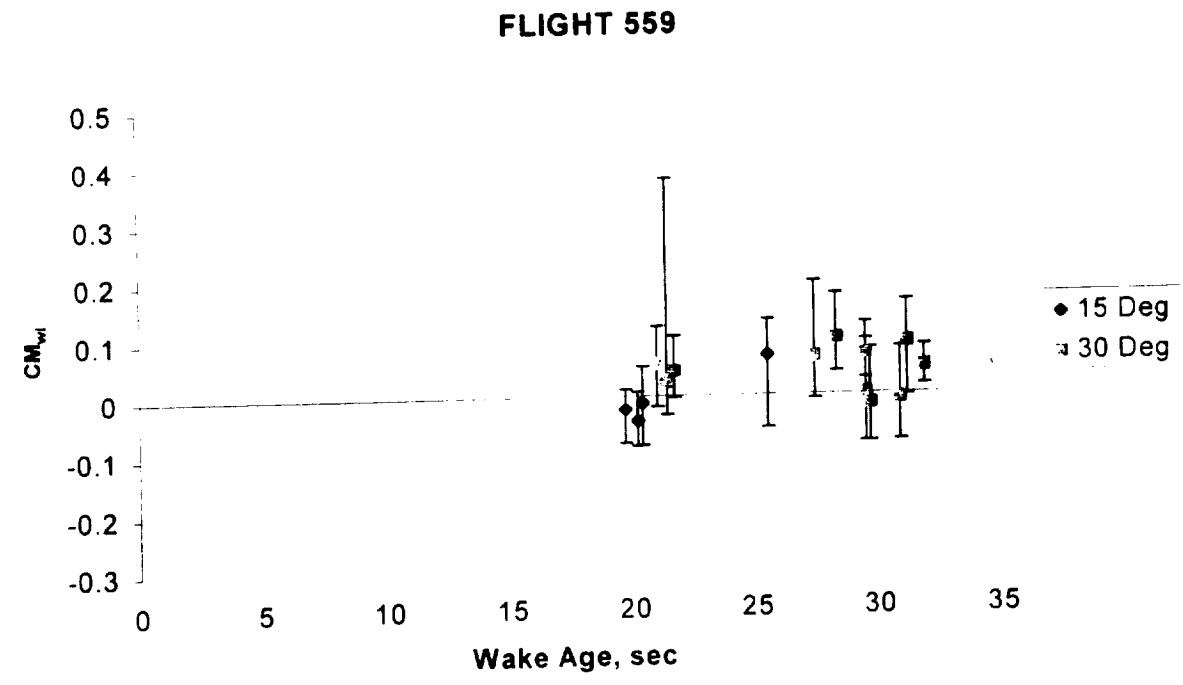

Figure 22: Wake-induced pitching moment coefficient, based on flap deflection.

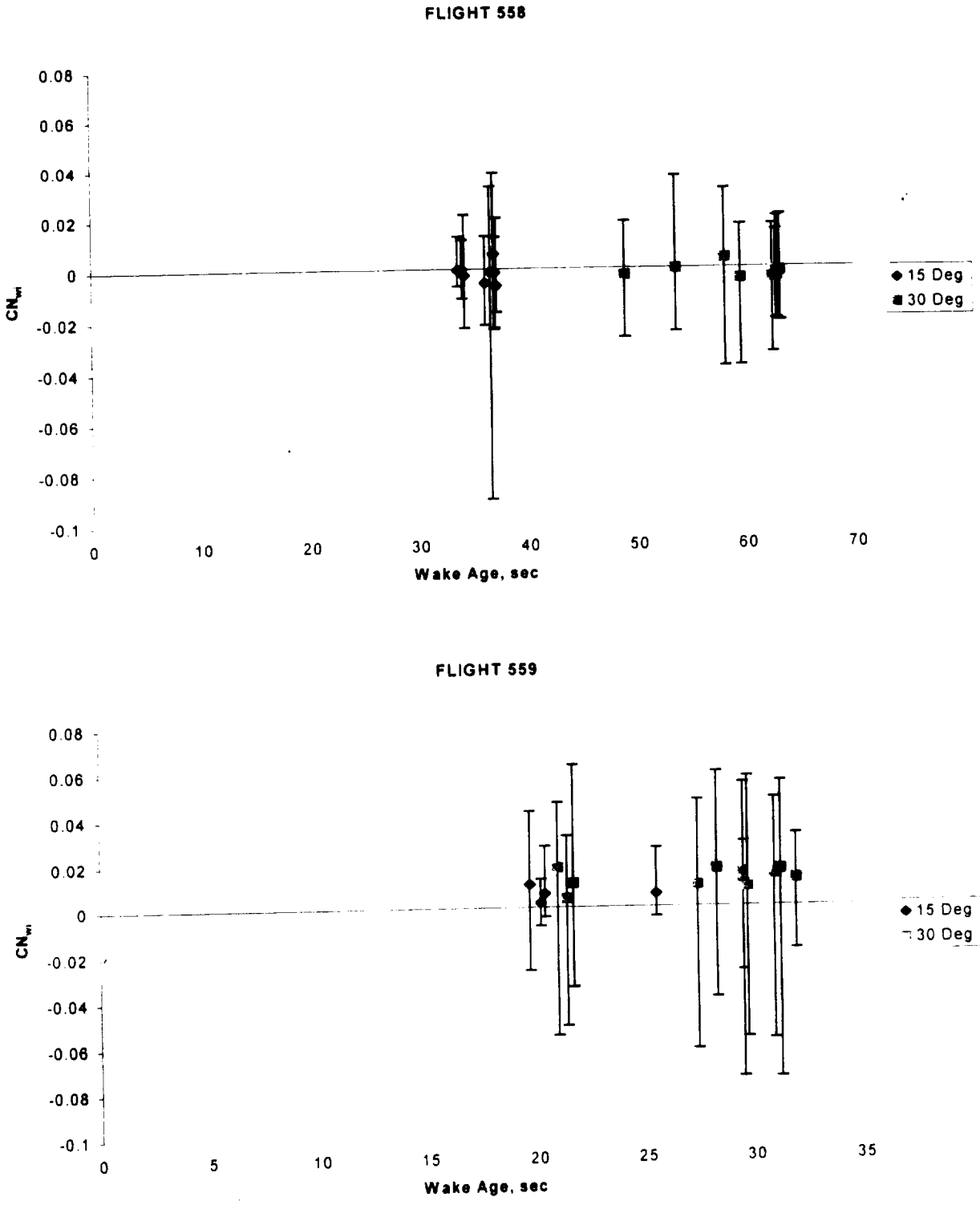

Figure 23: Wake-induced yawing moment coefficient, based on flap deflection.

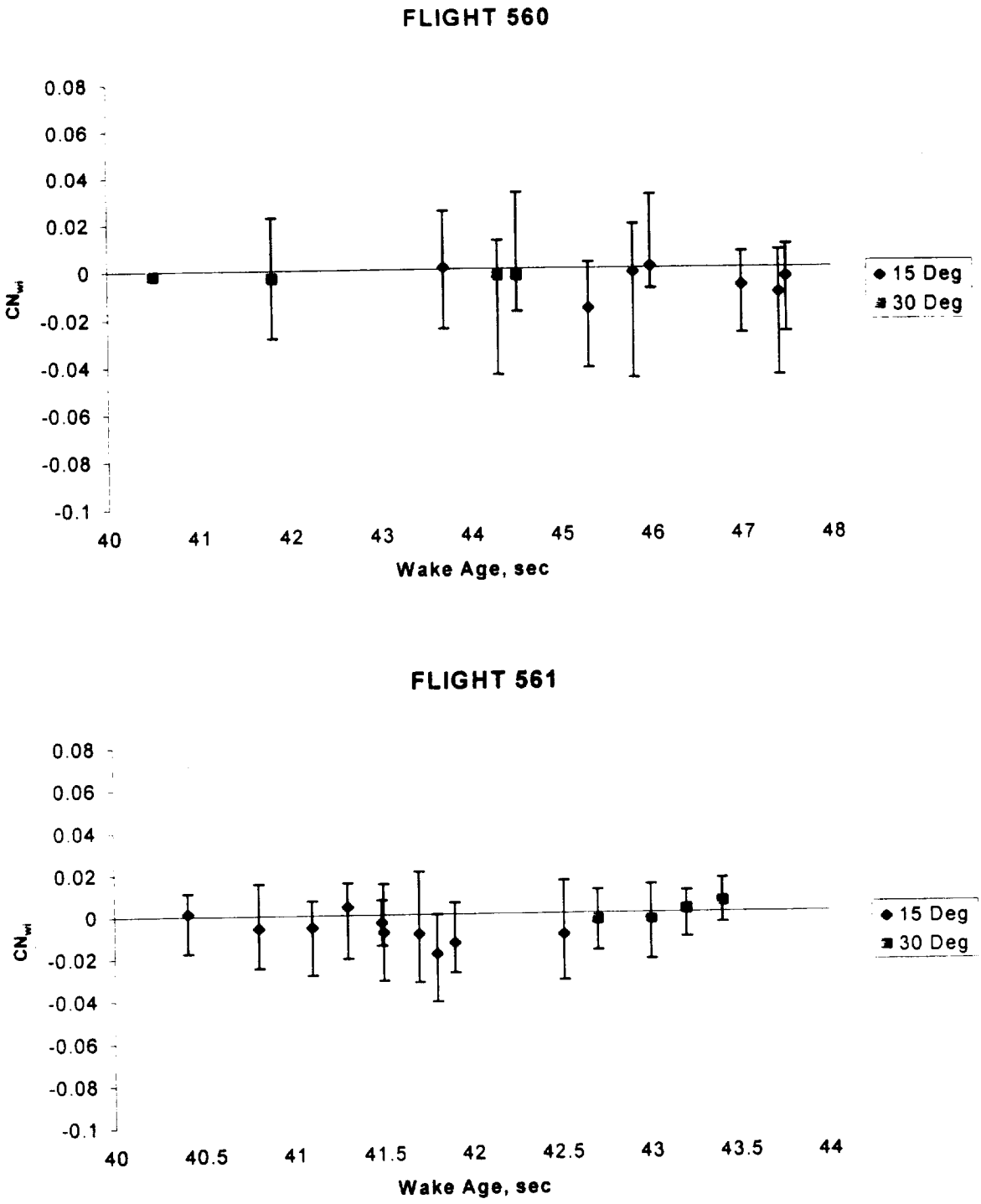

Figure 24: Wake-induced yawing moment coefficient, based on flap deflection.

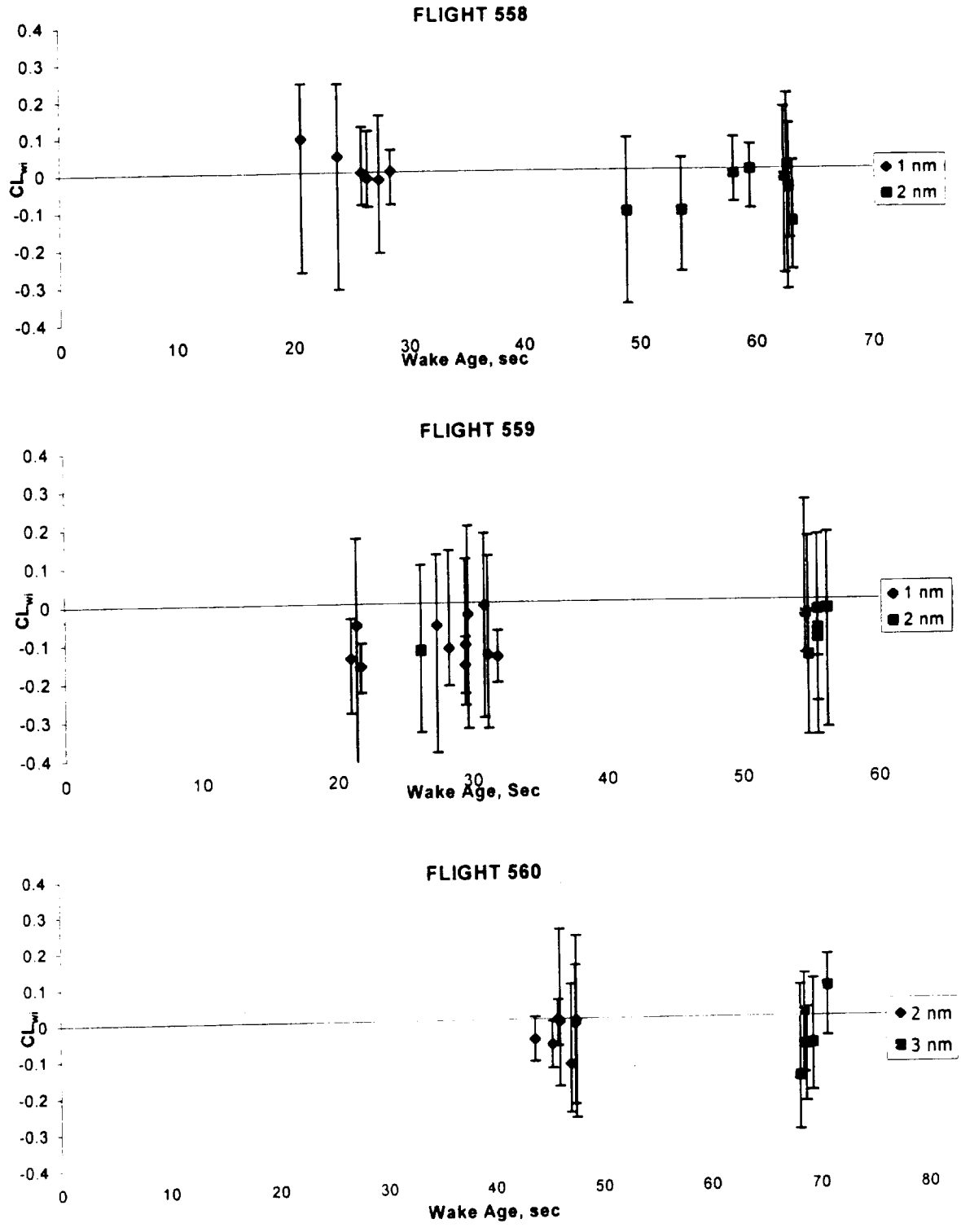

Figure 25: Wake-induced lift coefficient, based on separation distance.

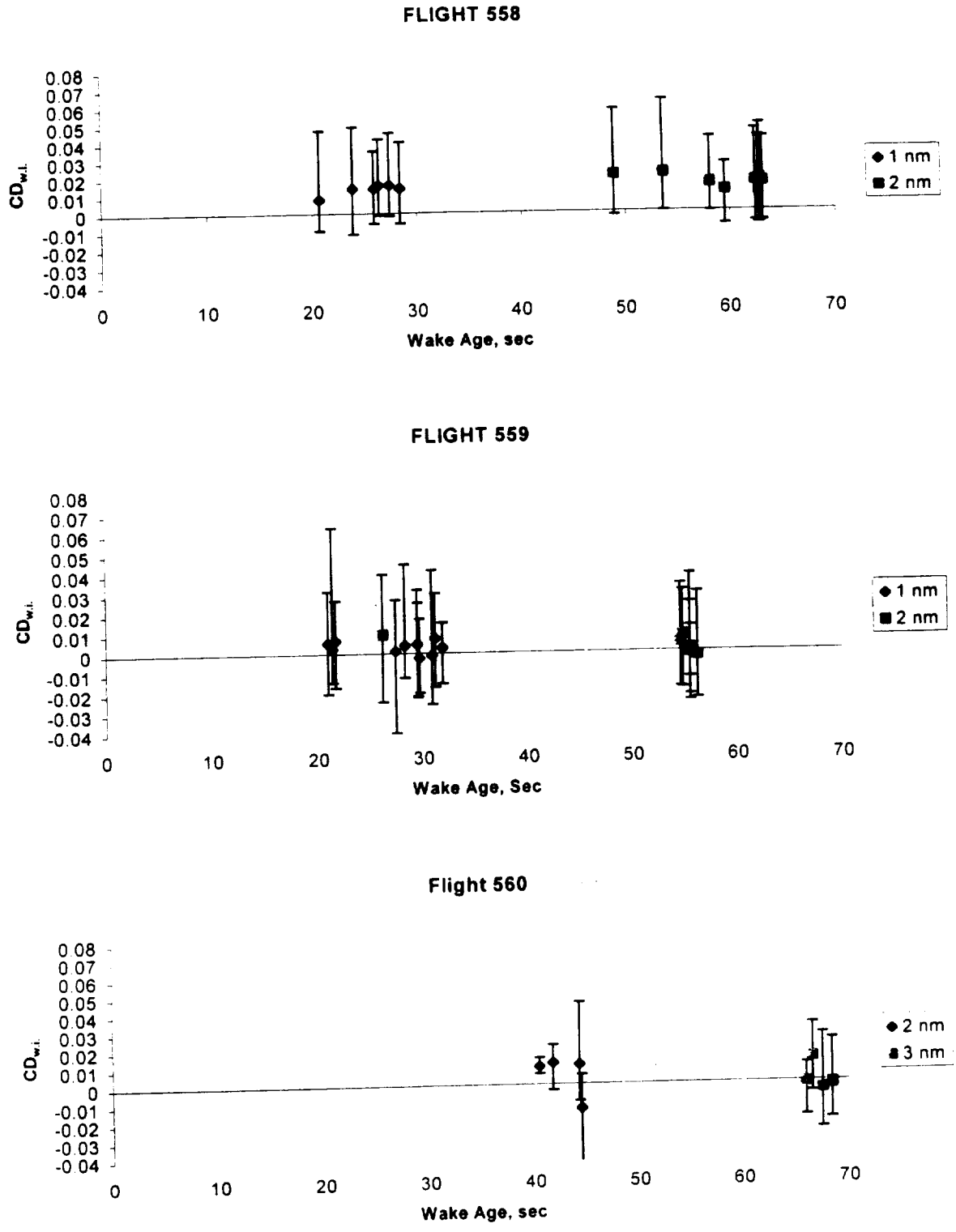

Figure 26: Wake-induced drag coefficient, based on separation distance.

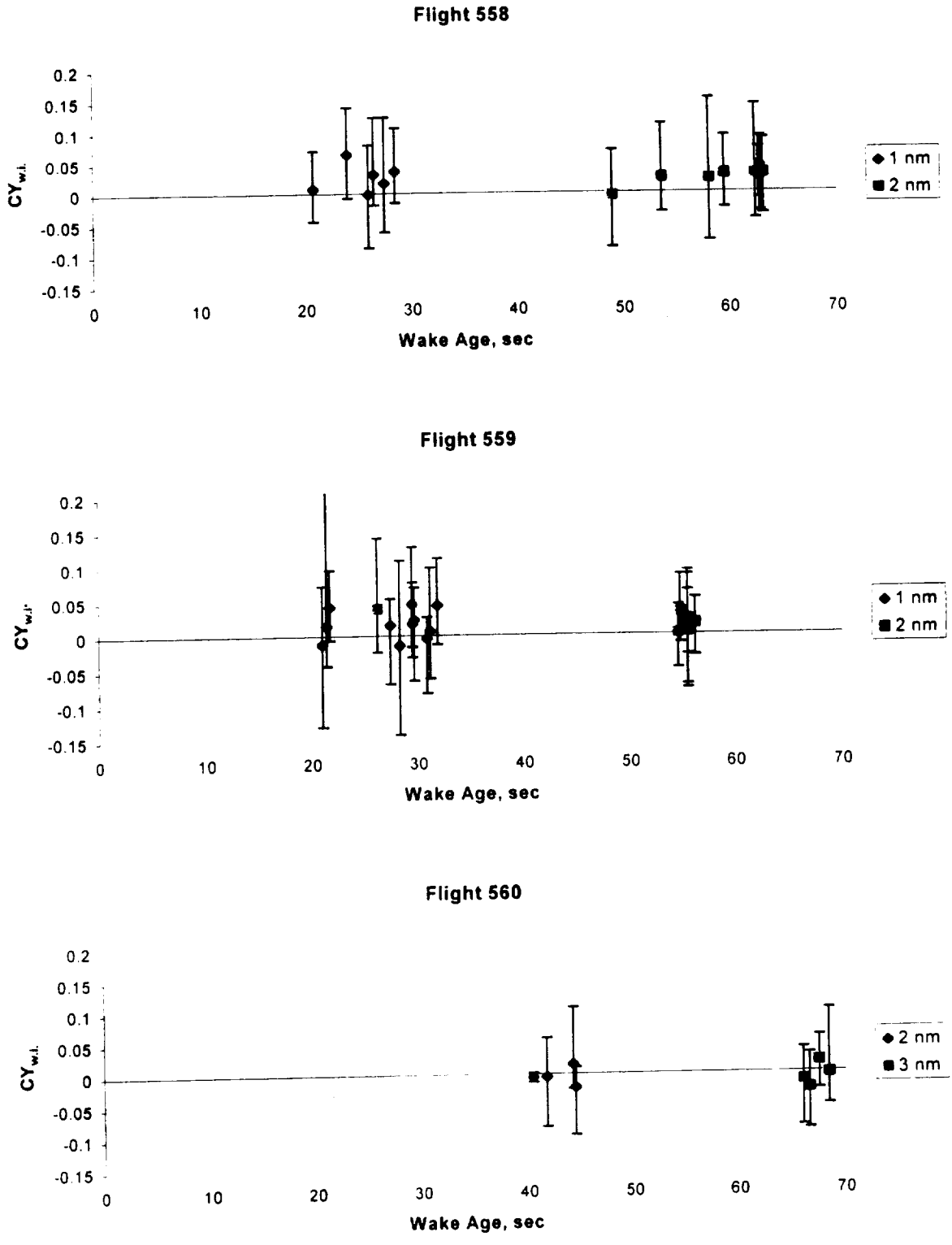

Figure 27: Wake-induced sideforce coefficient, based on separation distance.

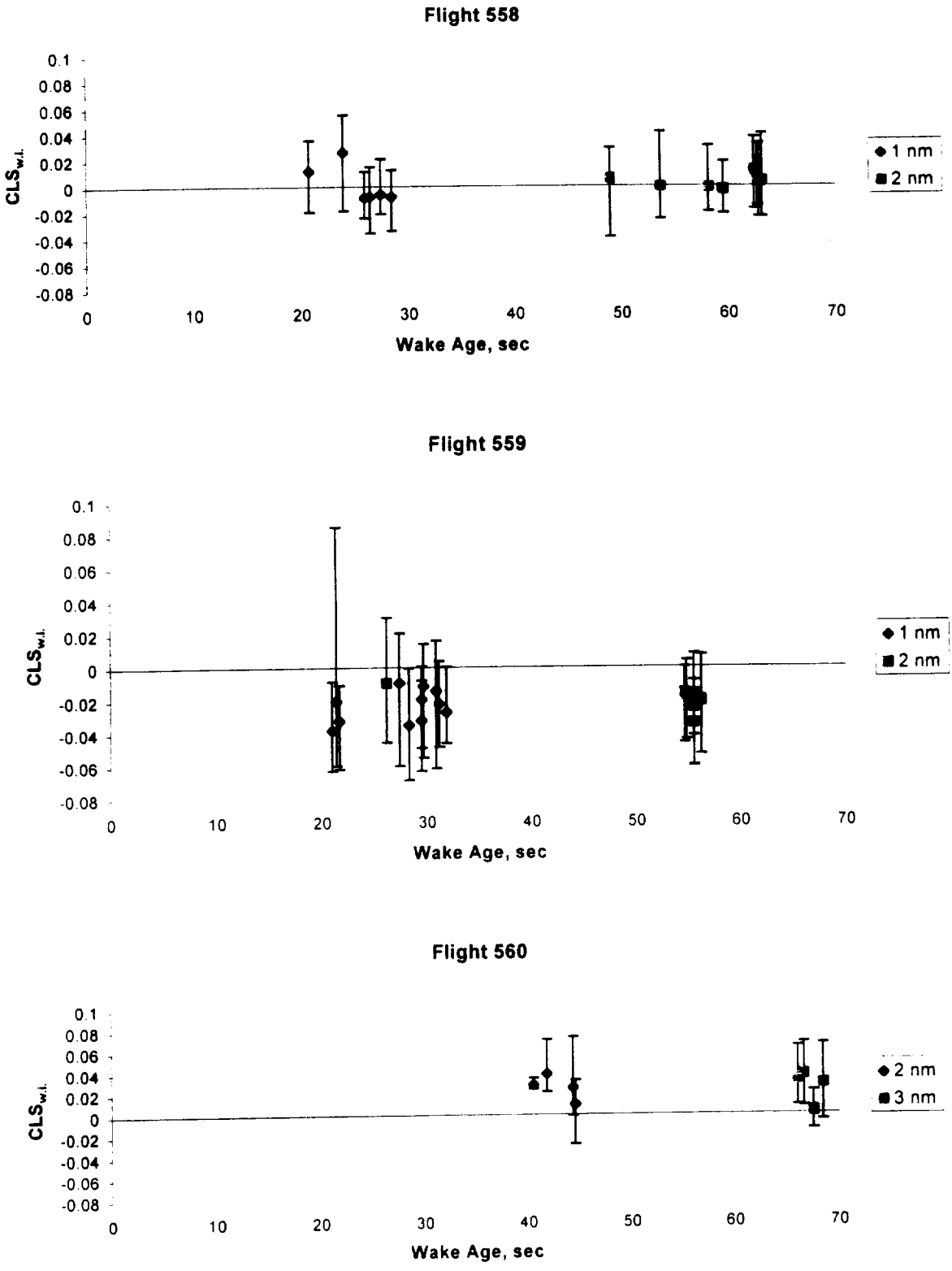

Figure 28: Wake-induced rolling moment coefficient, based on separation distance.

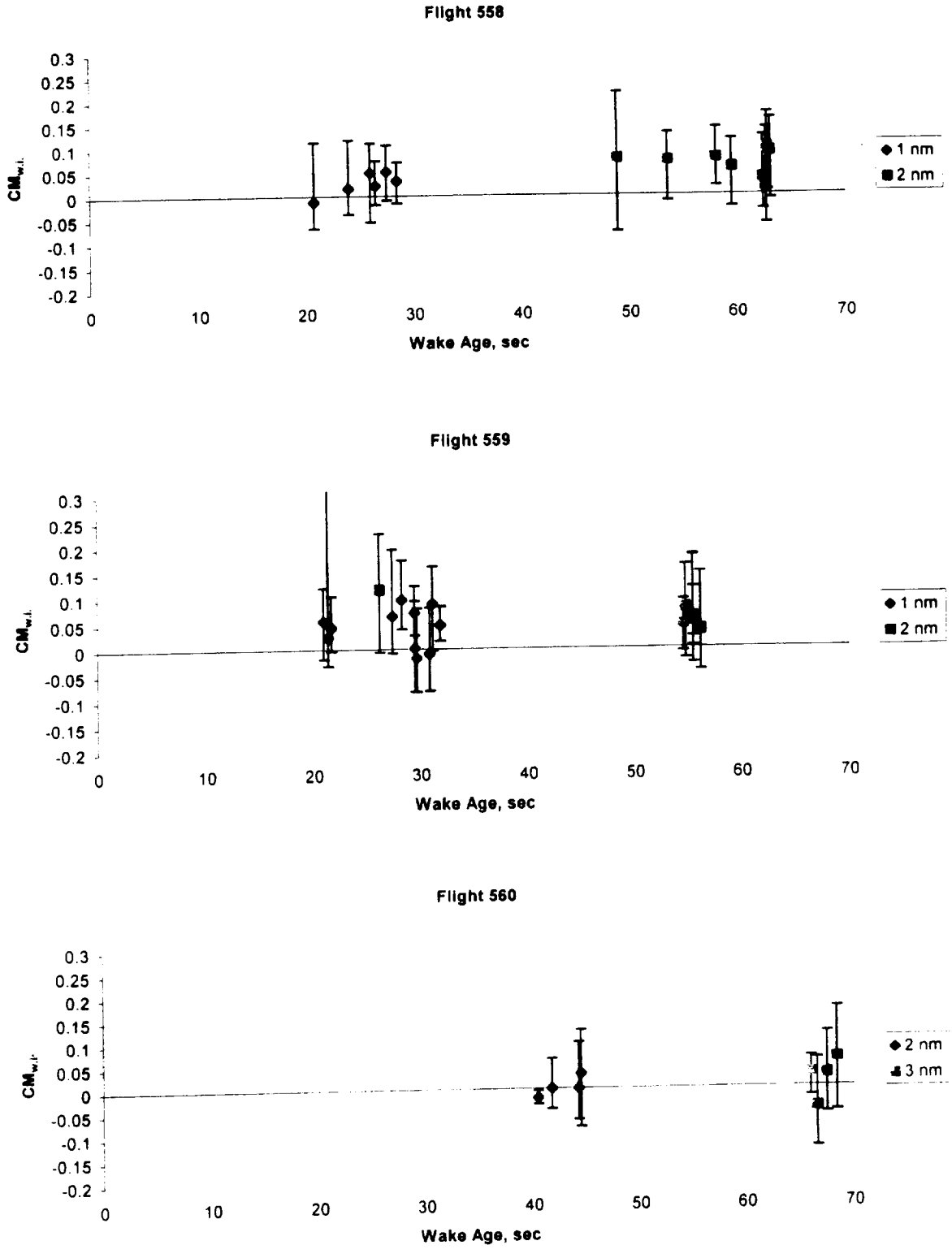

Figure 29: Wake-induced pitching moment coefficient, based on separation distance.

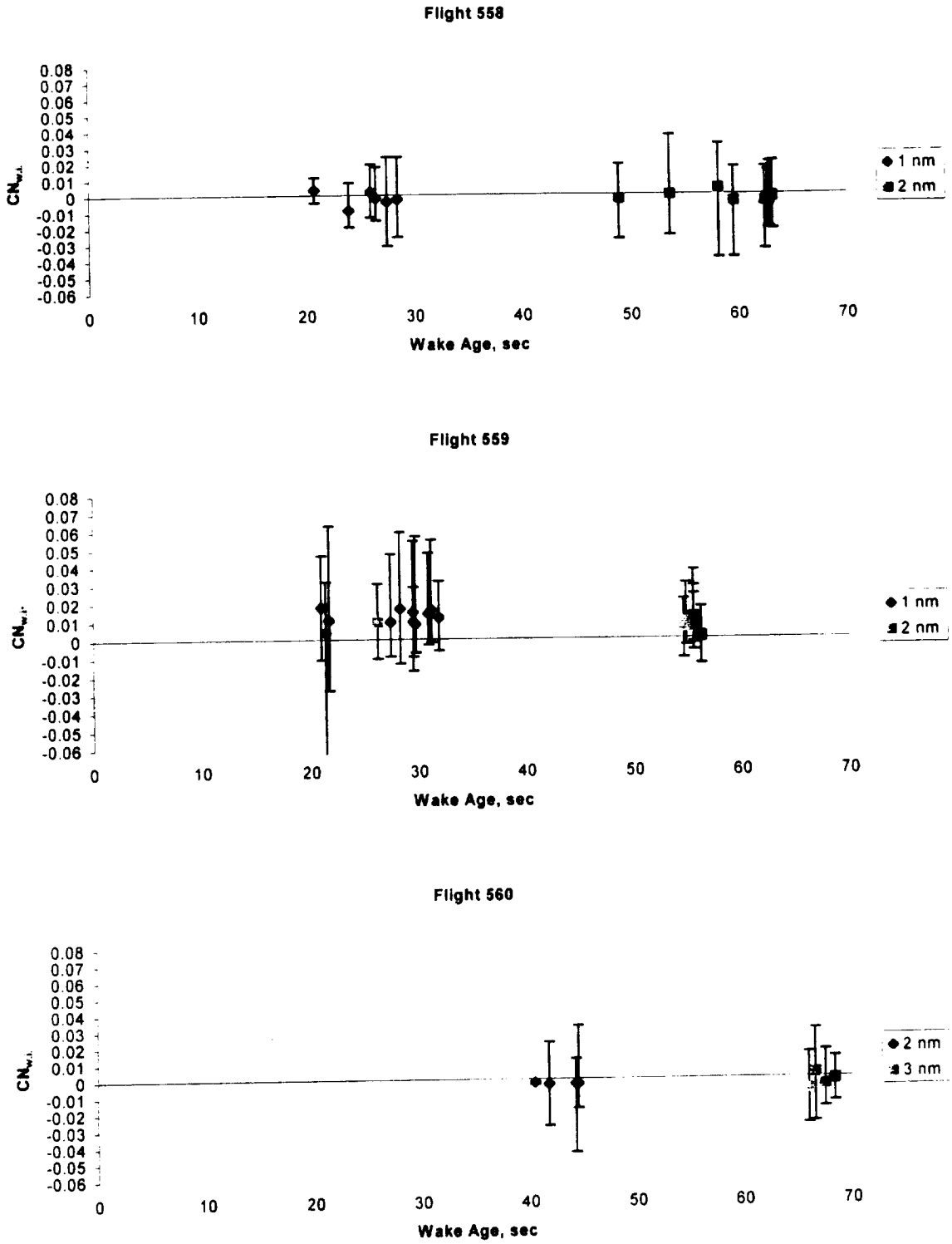

Figure 30: Wake-induced yawing moment coefficient, based on separation distance.

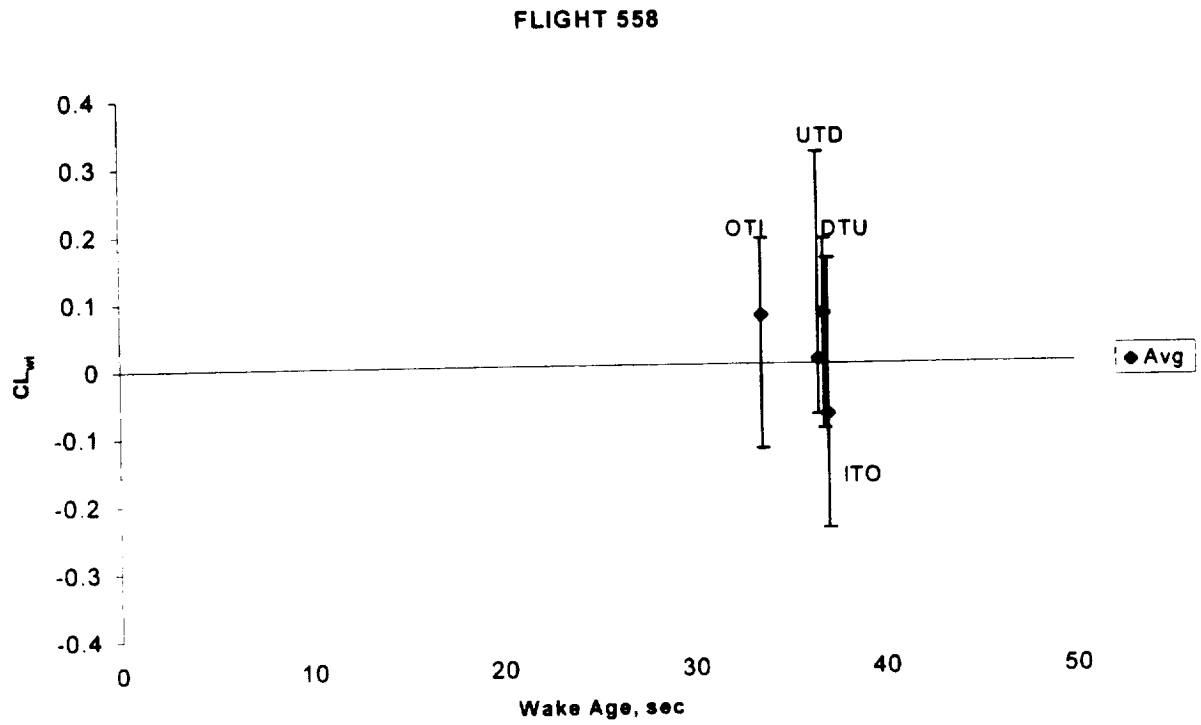

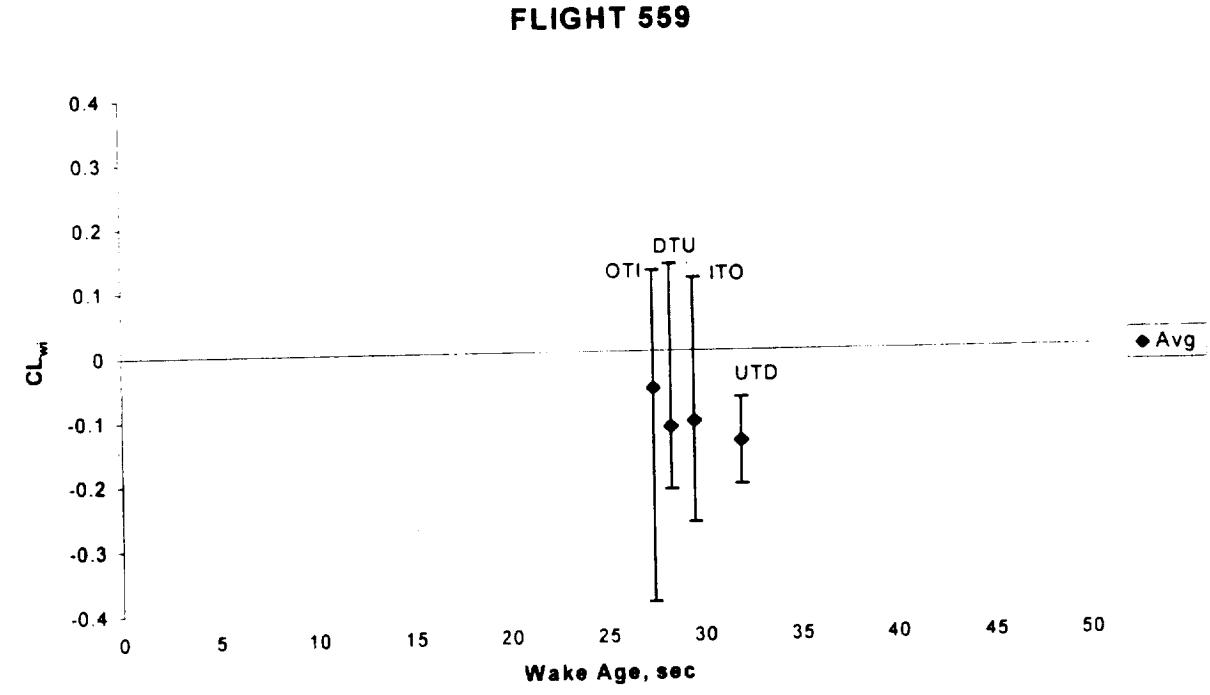

Figure 31: Wake-induced lift coefficient, based on flight maneuver.

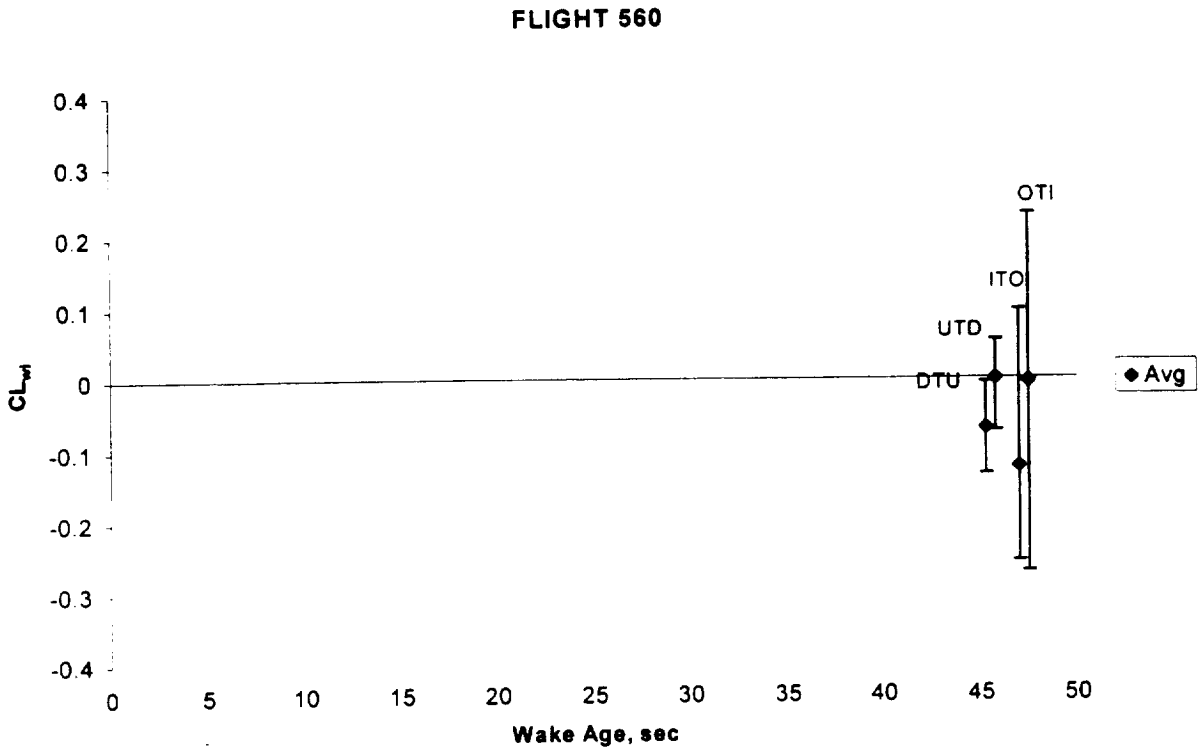

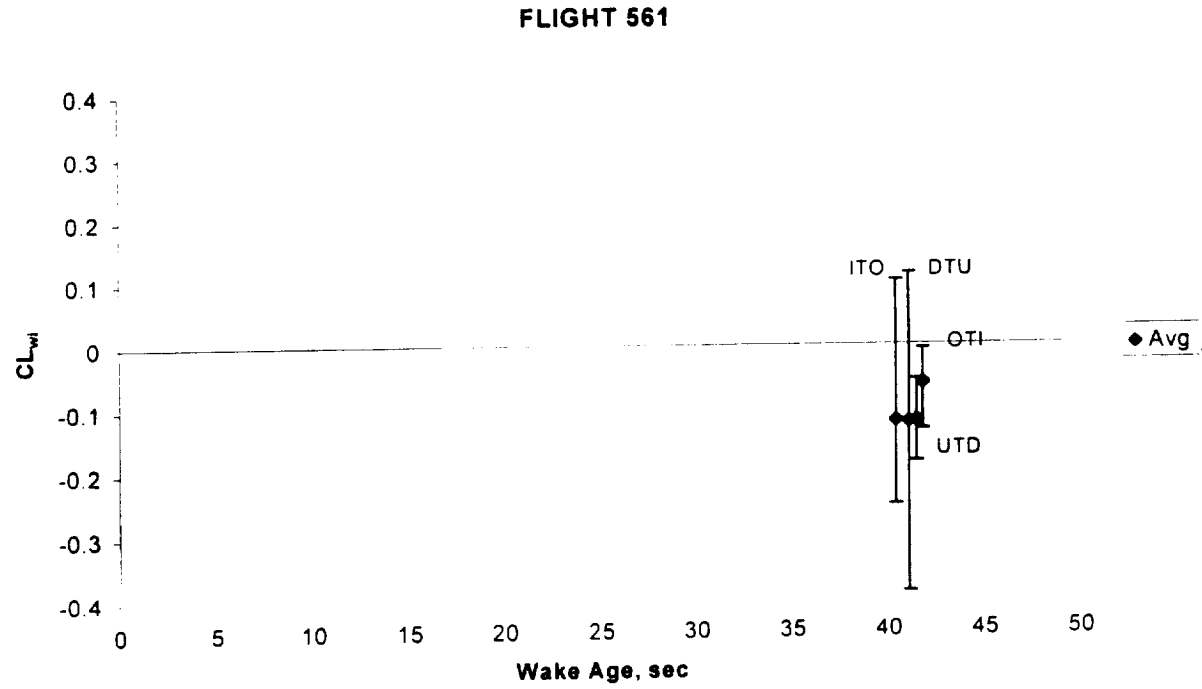

Figure 32: Wake-induced lift coefficient, based on flight maneuver.

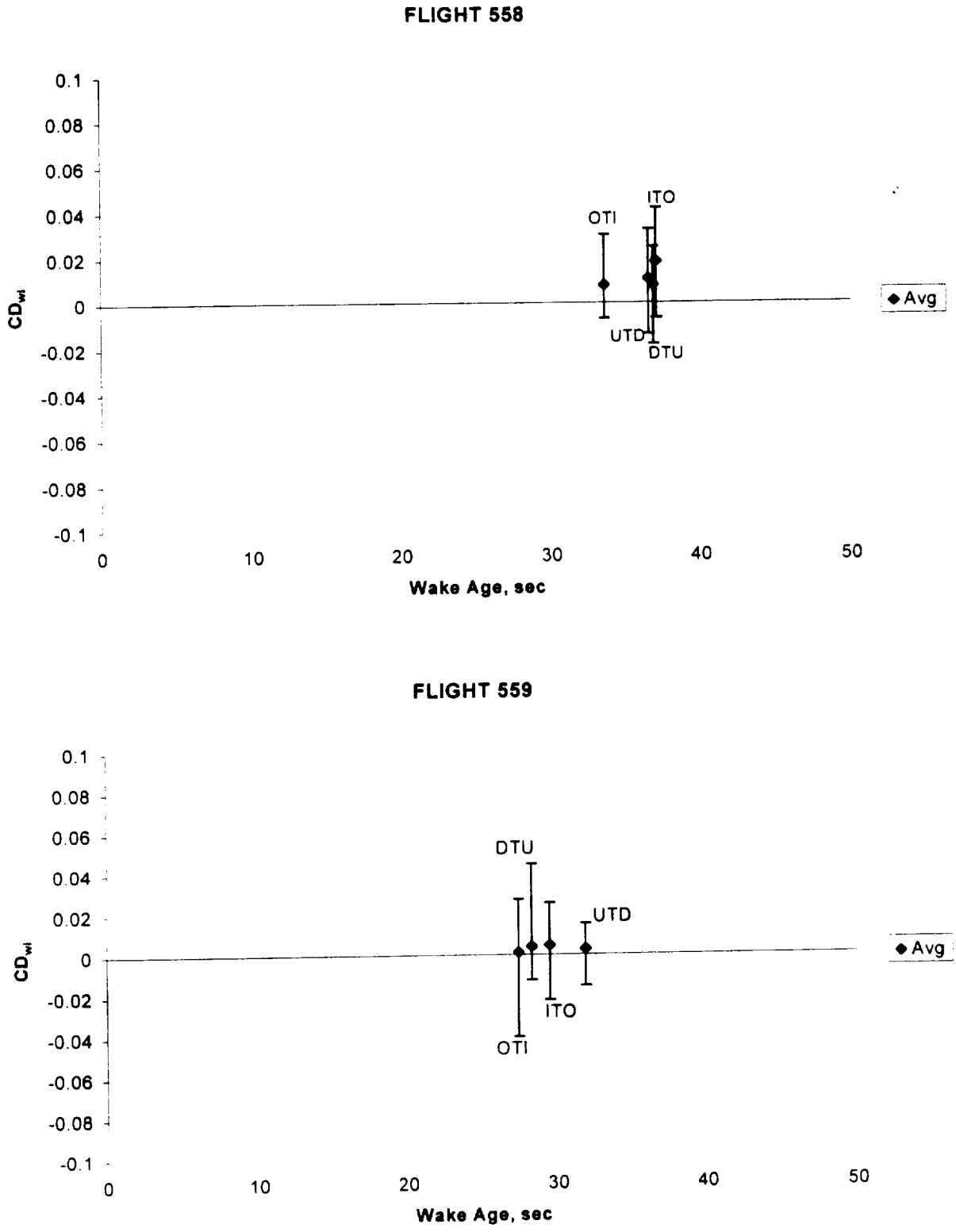

Figure 33: Wake-induced drag coefficient, based on flight maneuver.

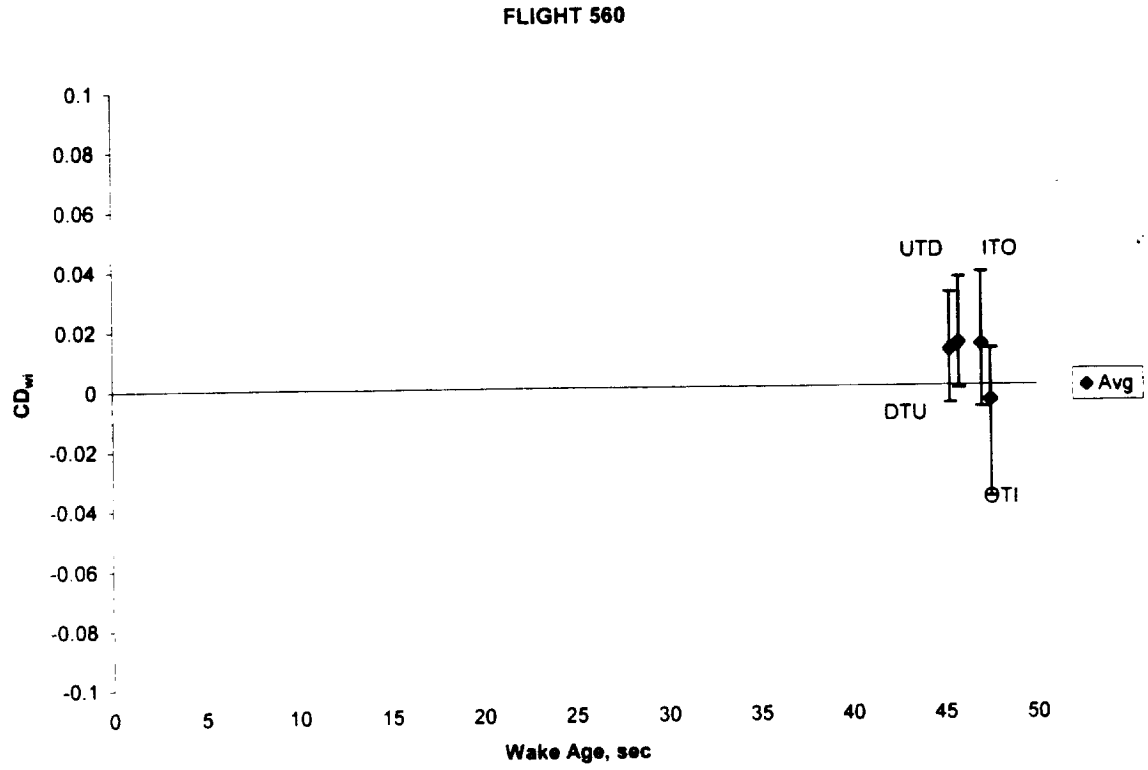

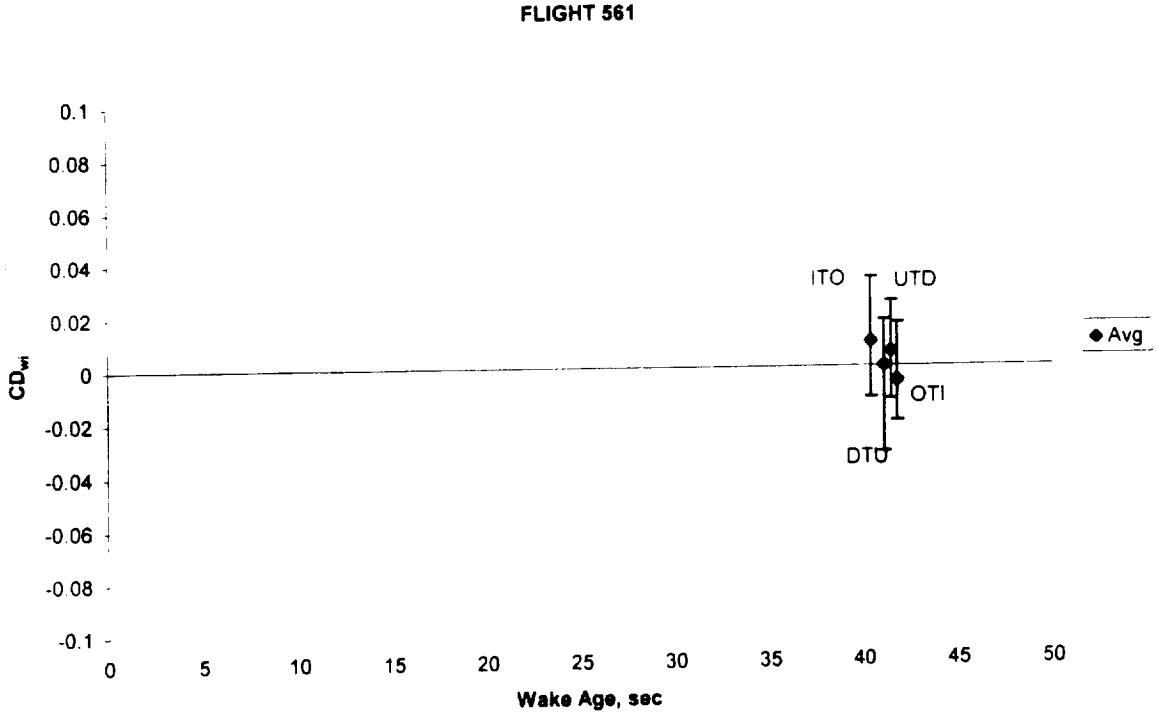

Figure 34: Wake-induced drag coefficient, based on flight maneuver.

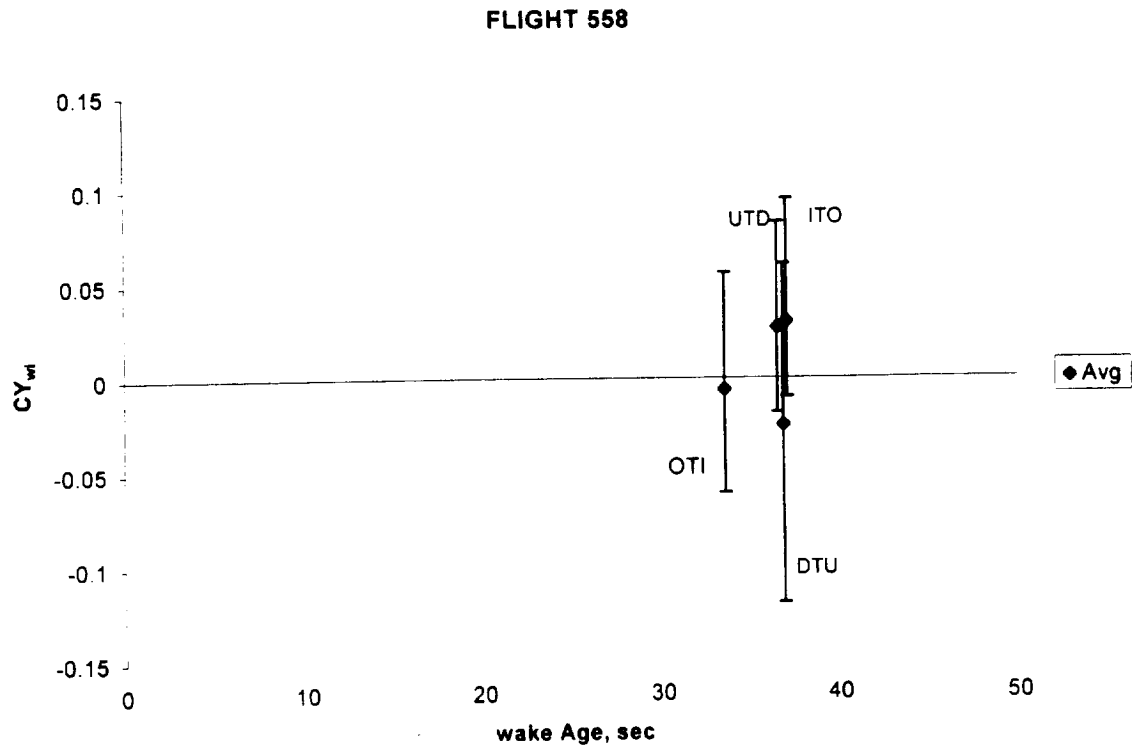

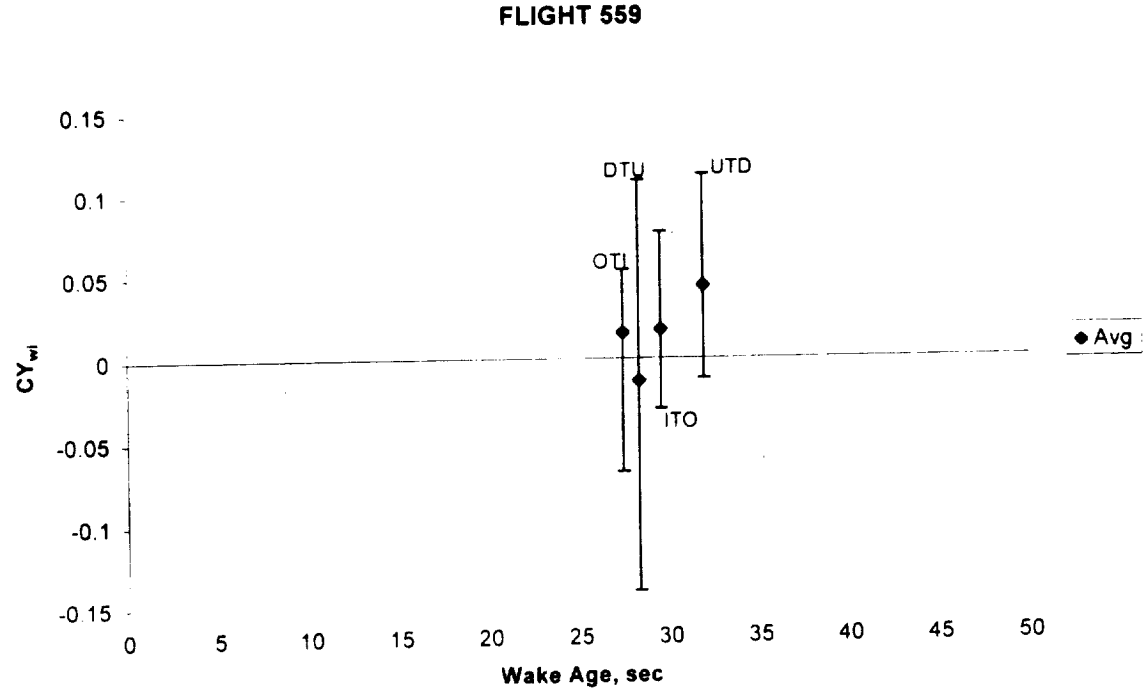

Figure 35: Wake-induced sideforce coefficient, based on flight maneuver.

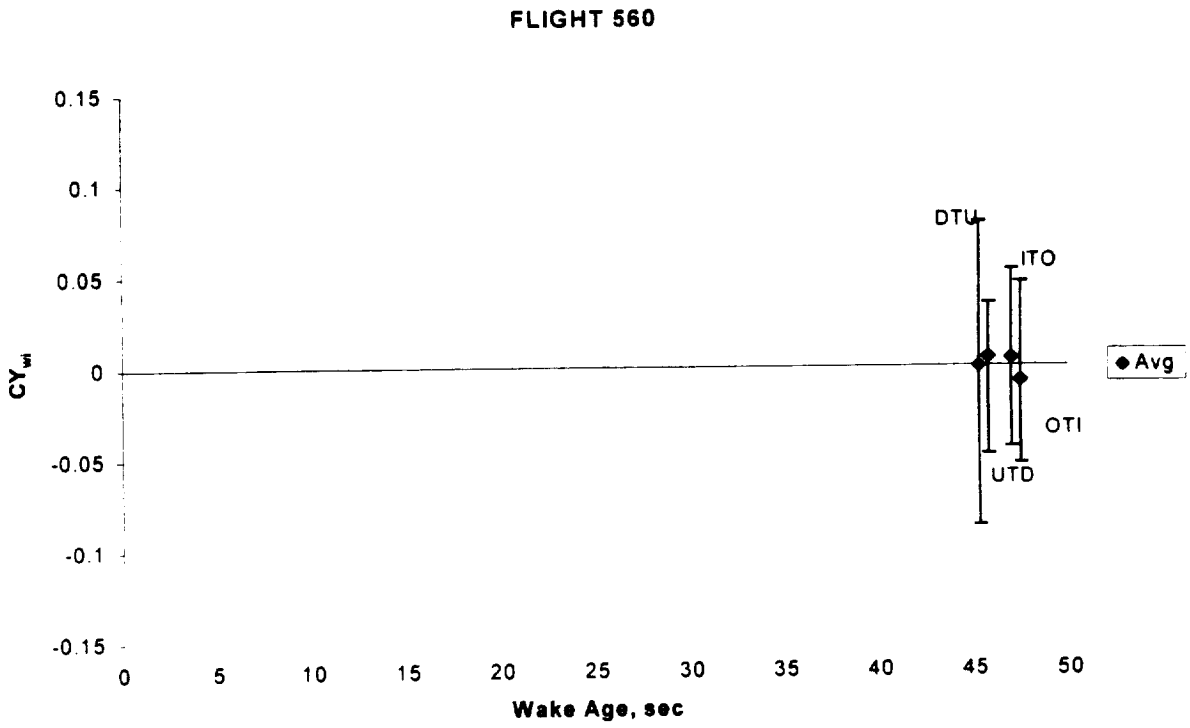

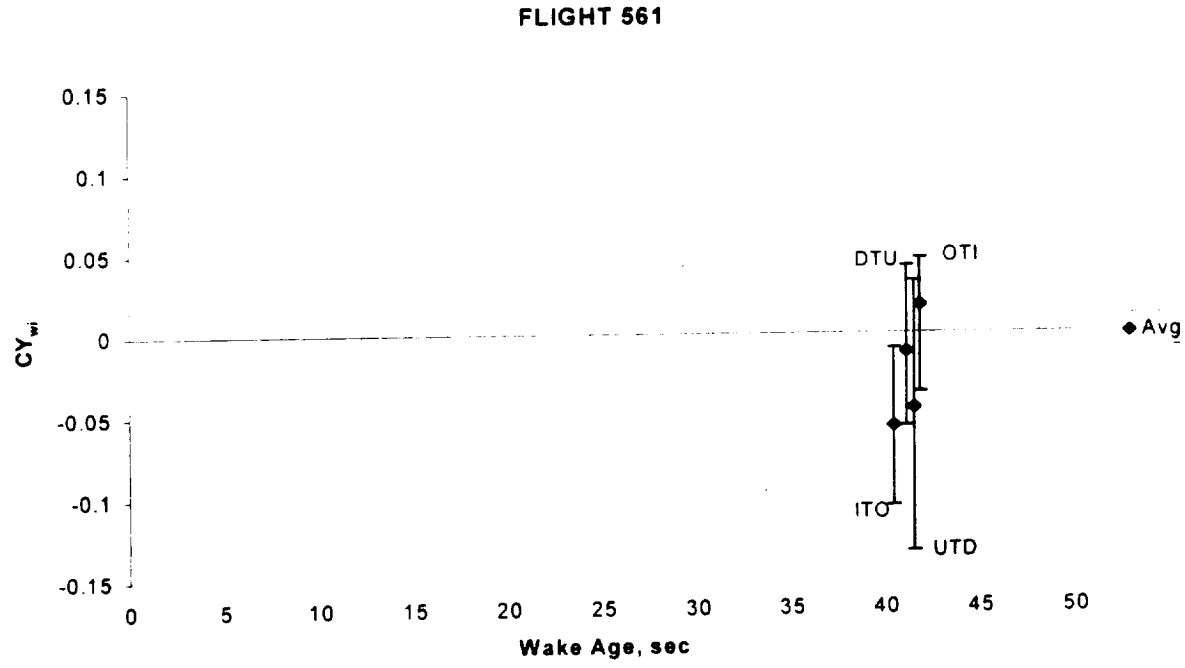

Figure 36: Wake-induced sideforce coefficient, based on flight maneuver.

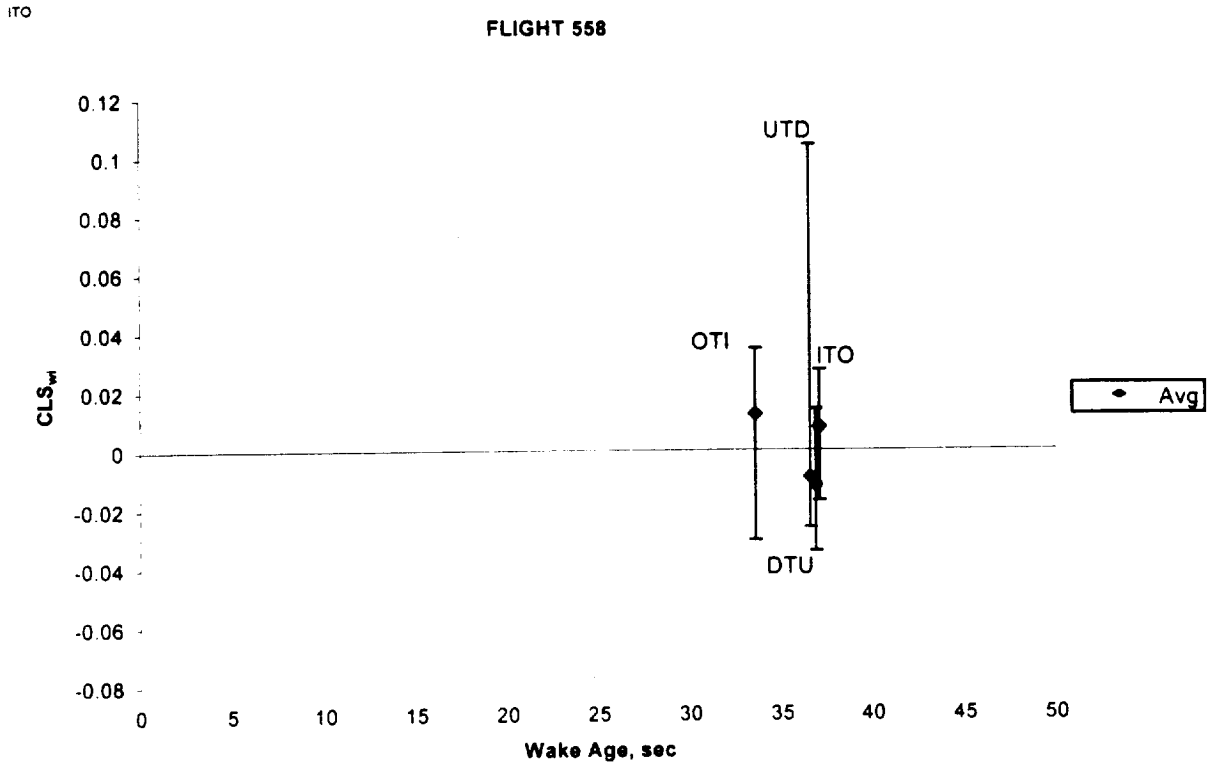

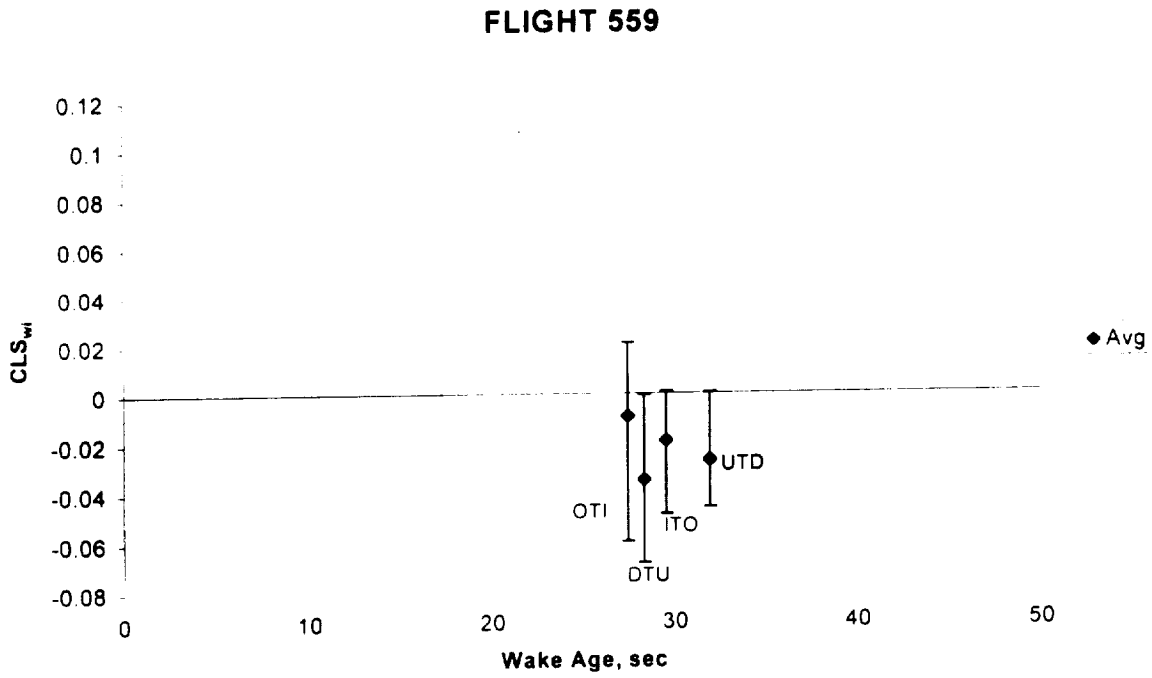

Figure 37: Wake-induced rolling moment coefficient, based on flight maneuver.

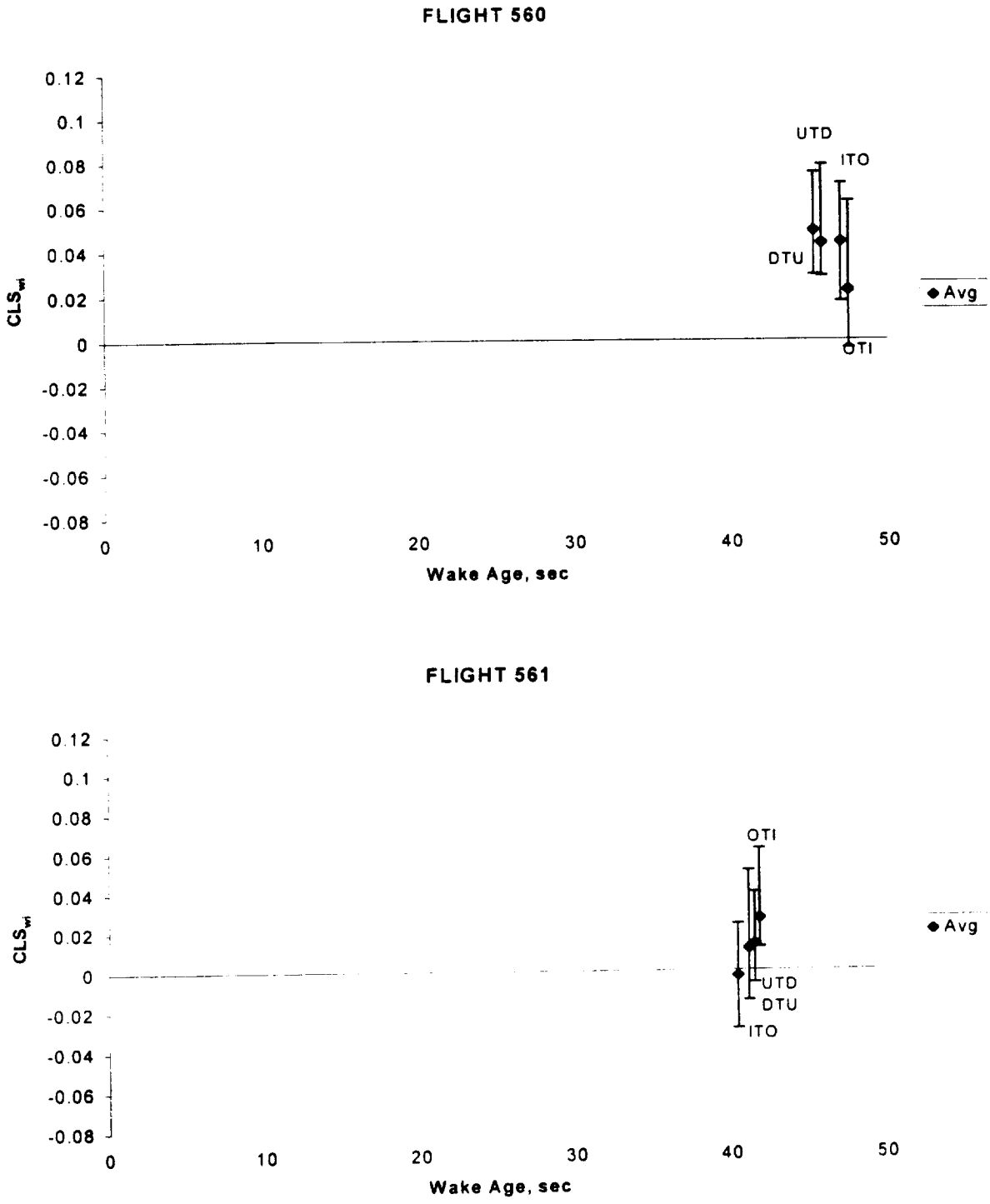

Figure 38: Wake-induced rolling moment coefficient, based on flight maneuver.

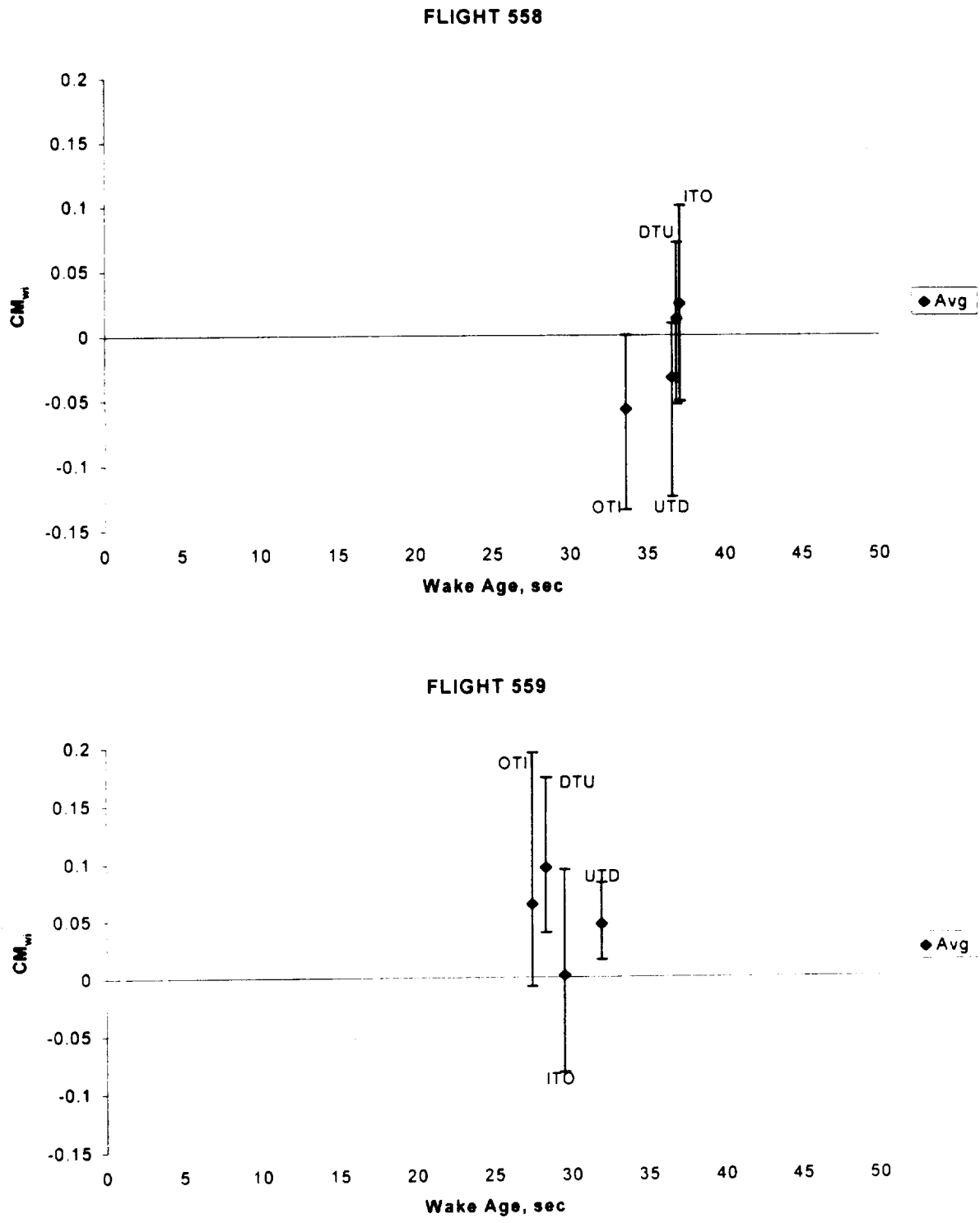

Figure 39: Wake-induced pitching moment coefficient, based on flight maneuver.

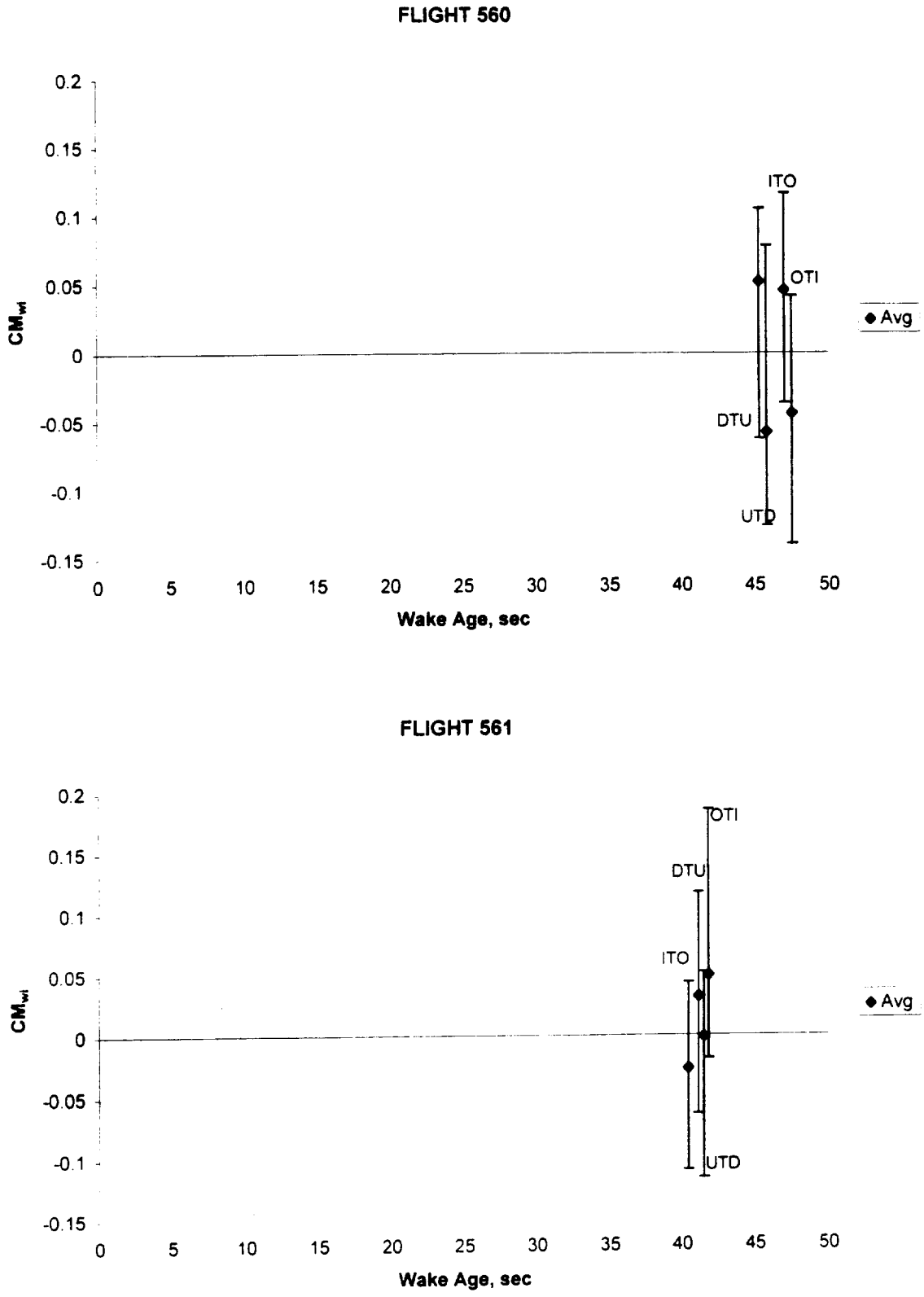

Figure 40: Wake-induced pitching moment coefficient, based on flight maneuver.

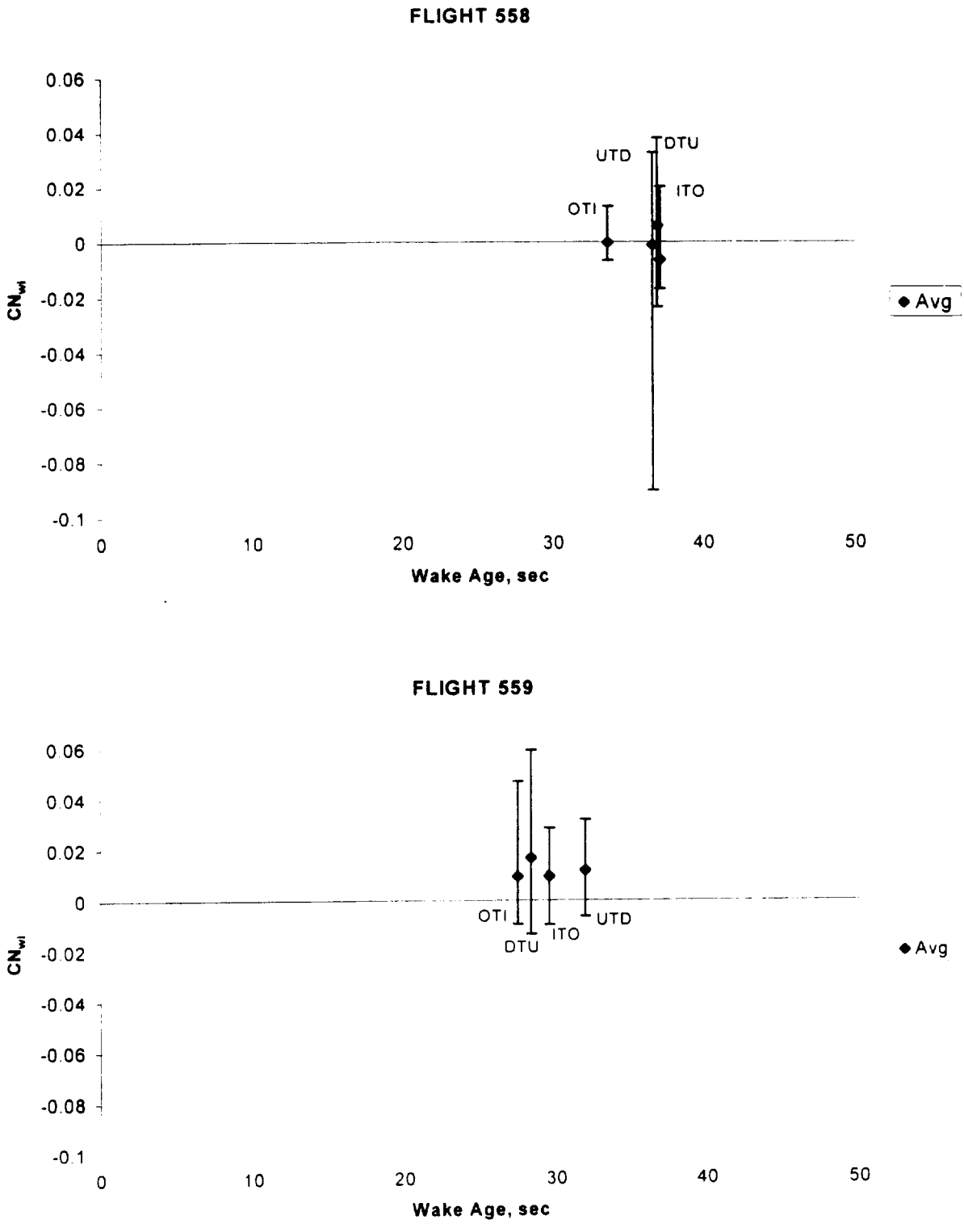

Figure 41: Wake-induced yawing moment coefficient, based on flight maneuver.

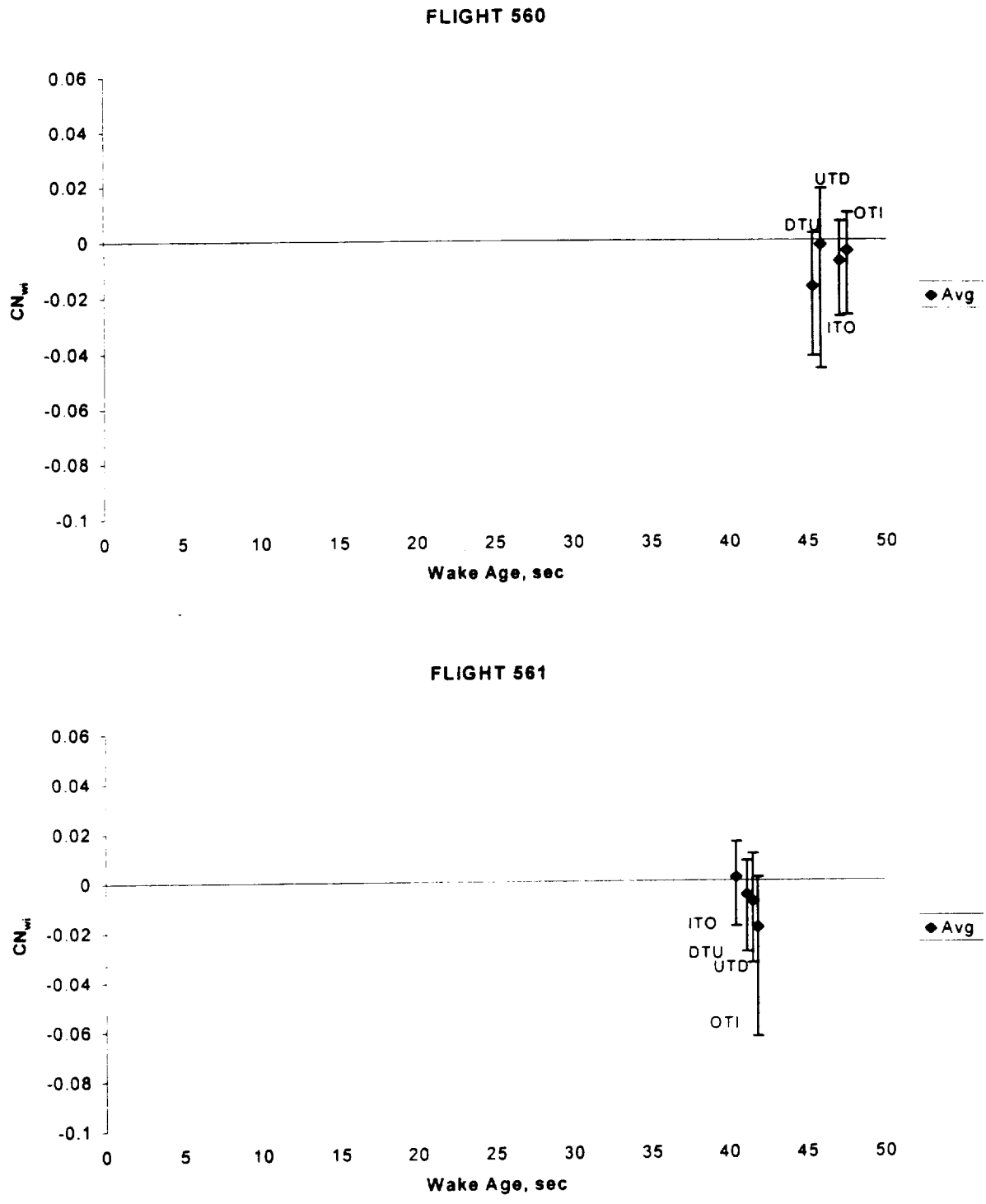

Figure 42: Wake-induced yawing moment coefficient, based on flight maneuver.

REFERNCES

1. Durham, R.E.; Stuever, R.A.; and Vicroy, D.D.: "The Challenges of Simulating Wake Vortex Encounters and Assessing Separation Criteria," AIAA Atmospheric Flight Mechanics Conference, August 9-11,1997; Monterey, CA.

2. Vicroy, D.; Brandon, J.; Greene, G.; River, R.; Stewart, E.; and Stuever, R.: "Characterizing the Hazard of a Wake Vortex Encounter," AIAA97-0055, 35th Aerospace Sciences Meeting & Exhibit, January 9-10,1997, Reno, NV.

3. Reimer, Heidi M.; and Vicroy, Dan D.: "A Preliminary Study of a Wake Vortex Encounter Hazard for a B737-100 Airplane," NASA TM 110223, April1996.

4. Hinton, D.A.: "An Aircraft Vortex Spacing System (AVOSS) for Dynamical Wake Vortex Spacing Criteria," AGARD 78TH Fluid Dynamics Panel Meeting and Symposium on the Characterization & Modification of Wakes From Lifting Vehicles on Fluids, May 20-23, Trundheim, Norway.

5. Greene, George C.: "An Approximate Model of Vortex Decay in the Atmosphere," *Journal of Aircraft*, Vol. 23, No.3, July 1986, pp. 566-573.

6. Corjon, Alexandre; and Poinsot, Thierry: "A Model to Define Aircraft Separations Due to Wake Vortex Encounter," AIAA95-1776-CP, pp.117-124.

7. Janota, Paul; Coburn, Allen R.; Thokar, Gregory A.; and Osovski, Lynne: "Relationship Between Wake Vortex Decay and Atmospheric Variable," A96-14212, 6th Conference on Aviation Weather Systems, pp. 161-165.

8. Ash, Robert L.; Zheng, Z. Charlie; Greene, George C.: "Cross Wind Effects on Turbulent Aircraft Wake Vortices Near the Ground," 25th AIAA Fluid Dynamics Conference, June 20-23, 1994; Colorado Springs, CO.

9. Sammonds, Robert I.; Stinnett, Glen W.; and Larsen, William E.: "Criteria Relating Wake Vortex Encounter Hazard to Aircraft Response," *Journal of Aircraft*, Vol.14, No. 10, October 1977, pp. 981-987.

10. Rossow, Vernon J.; and Tinling, Bruce E.: "Research on Aircraft/ Vortex-Wake Interactions to Determine Acceptable Level of Wake Intensity," *Journal of Aircraft*, Vol. 25, No. 6, June 1998,pp. 481-492.

11. Stuever, R.A.; and Greene, George C.: "An Analysis of Relative Wake vortex Hazards for Typical Transport Aircraft, " AIAA 94-0810, January 1994.

63

12. Stewart, E. C.: "A Study of the Interaction Between A Wake Vortex and an Encountering Airplane," AIAA-93-3642-CP, pp. 258-267.

13. Walden, A. B.; van Dam, C. P.; and Brandon, J. M.: "Modeling of the Interaction Between a Lifting Wing and a Following Aircraft and Comparisons with Experimental Results," AIAA-9690771, 34th AIAA Aerospace Sciences Meeting and Exhibit, January 1996; Reno, NV.

14. Brandon, Jay M.; Jordan Jr., Frank L.; Stuever, Robert A.; and Buttrill, Catherine W.: "Application of Wind Tunnel Free-Flight technique for Wake Vortex Encounters," NASA TP3672, November 1997.

15. Vicroy, Dan D.; and Nguyen, Truc: "A Numerical Simulation Study to Develop an Acceptable Wake Encounter Boundary for a B737-100 Airplane," AIAA-96-3372-CP, pp. 88-96.

16. Stuever, Robert A.; Stewart, Eric C.; and Rivers, Robert A.: "Overview of the Preparation and Use of an OV-10 Aircraft for Wake Vortex Hazards Flight Experiments," 1st AIAA Aircraft Engineering, Technology, and Operations Congress, September 19-21, 1995; Los Angeles, CA.

17. Vicroy, Dan D.; Vijon, Paul M.; Reimer, Heidi M.; Gallegos, Joey L.; and Spalart, Phillippe R.: "Recent NASA Wake-Vortex Flight Test, Flow Physics Database and Wake Development Analysis," 1998 World Aviation Conference, September 28-30, 1998; Anaheim, CA.

18. Perry, R. Brad; Hinton, David A.; and Stuever, Robert A.: "NASA Wake Vortex Research for Aircraft Spacing," AIAA 97-0057, 35th Aerospace Sciences Meeting and Exhibit, January 6-10, 1997; Reno, NV.

19. Vicroy, Dan D.; Stuever, Eric C.; and Rivers, Robert A.: "Flight Reduction of Wake Velocity Measurements Using an Instrumented OV-10 Airplane," NASA TM –1999-209552, September 1999.

20. Gainer, Thomas G.; and Hoffman, Sherwood: "Summary of Transformation Equations and Equations of Motion Used in Free-Flight and Wind-Tunnel Data Reduction and Analysis," NASA SP-3070, 1972.

21. Aviation Fundamnetals. Sixth Edition. 1998. Englewood, CO. Jeppesen Sanderson, Inc.

22. Kermore, A.C. 1996. Mechanics of Flight. Tenth Edition. Essex, England. Longman Group Limited. Pp. 105-111.

23. Etkin, Bernard.1982. Dynamics of Flight: Stability and Control. Second Edition. New York. John Wiley and Sons, Inc. Pp. 2-11.

24. Russell, J.B. 1996. Performance and Stability of Aircraft. New York. John Wiley and Sons, Inc.

25. Pete, Kimberly. 1999. "Model Validation for Wake-Vortex/ Aircraft Encounters. Howard University.

APPENDIX 1

Coordinate Systems

In order to calculate the wake-induced force and moments imparted on the B737, it is necessary to discuss three coordinate systems: Earth axis, body axis, and flight stability. Each of these systems uses the right-hand rectangular Cartesian axes [20].

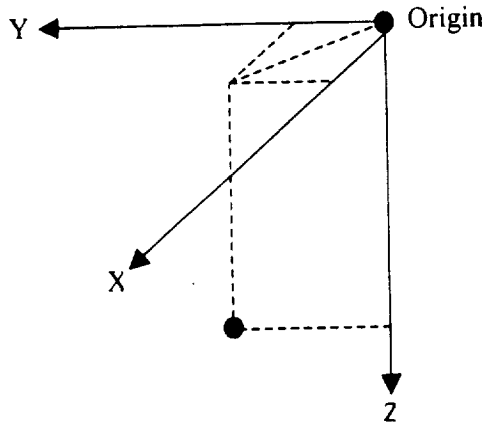

Figure A1: Right Hand Cartesian Coordinate System

The Earth, or inertial, axis system makes the assumption that the Earth is flat and nonrotating. The X and Y axes lie in the geometric plane of the Earth, with X pointing North and Y pointing East. The Z-axis points down towards the center of the Earth. The aircraft's velocity components were recorded with respect to this coordinate system.

In the body axis coordinate system, the rectangular Cartesian coordinates are fixed within the Boeing 737 aircraft at its center of gravity. The X-axis points out of the nose of the aircraft while the Y-axis is out the aircraft's right wing. The Z-axis is pointed downward and is perpendicular to both the X and Y-axis [20].

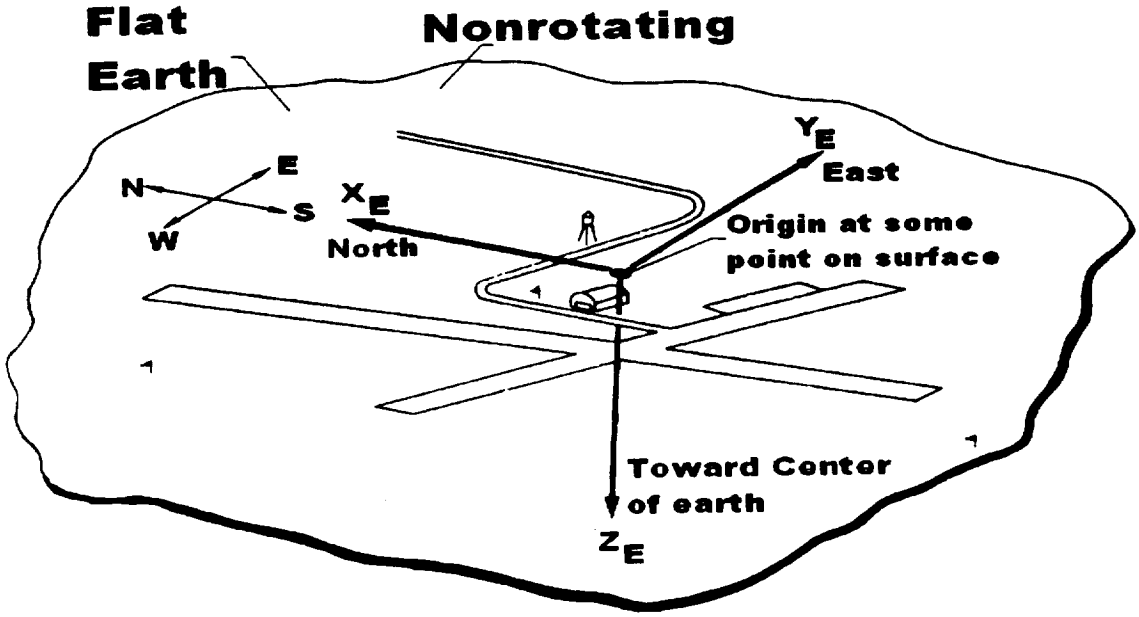

Figure A2: Earth axis system

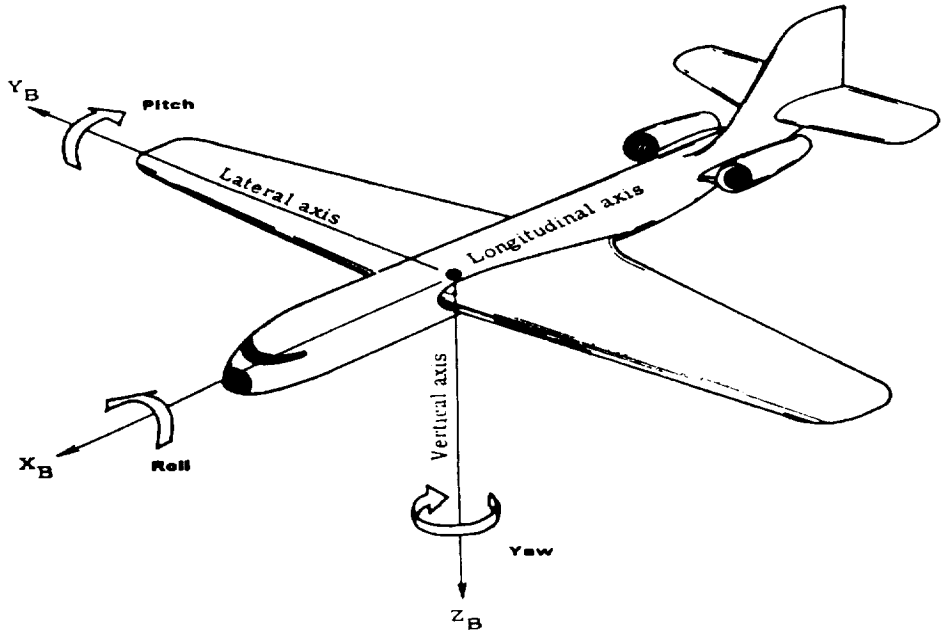

Figure A3: Body and stability axes systems

This final coordinate system used in this analysis is the flight stability system. It is fixed to the body coordinate system and is typically used when describing flight maneuvers [23]. The axes which makeup the flight stability system are the longitudinal, lateral, and vertical axes. A description of the motion about these axes is described below and in Figures A3-A4 [21].

Roll: The airplane rotates about its longitudinal, or X, axis. Positive roll is initiated when the aircraft's Y-axis turns towards the Z-axis. The ailerons produce this rolling motion.

Pitch: The airplane rotates about the lateral, or Y, axis. Positive pitch is achieved when the aircraft's Z-axis turns towards the X-axis. This causes the nose of the aircraft to rise. The horizontal stabilizer, or elevator, produces this motion.

Yaw: The airplane rotates about the vertical, or Z, axis. Positive yaw is achieved when the aircraft's X-axis turns toward the Y-axis. In this situation, the nose to moves the right or clockwise when viewed from above.

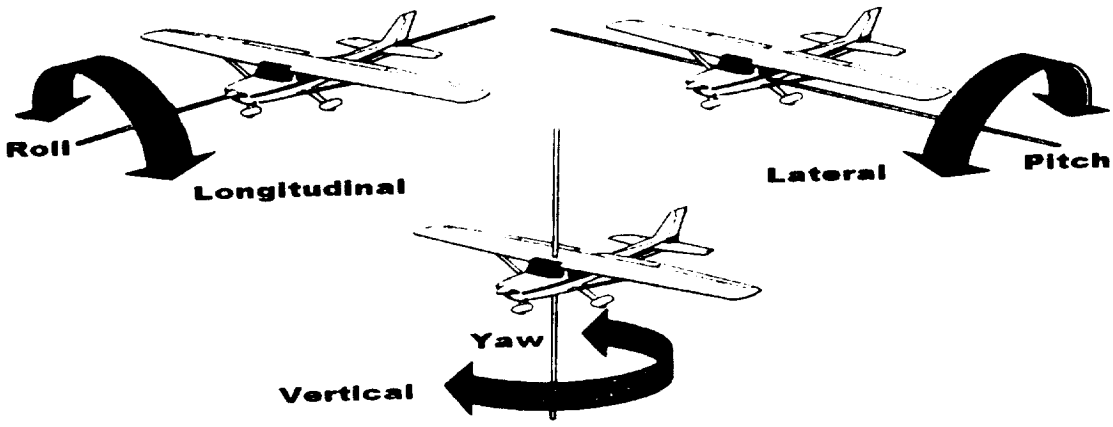

Figure A4: Stability axes

APPENDIX II

Mapping of Simulation Variables to the Flight Data Variables

Sim. Var.	Flt. Var.	Description	Units
P	ROLL_RTE_A	Roll Rate	degrees/sec
Q	PITCH_RTE_A	Pitch Rate	degrees/sec
R	YAW_RTE_A	Yaw Rate	degrees/sec
ALPHA	*	Attack Angle	degrees
ALPDOT	*	Rate change of Attack Angle	degrees/sec
BETA	*	Sideslip Angle	degrees
BETADOT	*	Rate change of Sideslip Angle	degrees/sec
SPL	SPLR_2	Left Spoiler Deflection	degrees
SPR	SPLRL_7	Right Spoiler Deflection	degrees
DLHDEG	STAB_TRIM	Horiz. Stabilizer Deflection	degrees
DLFDEG	FLAP_POS	Flap Position	degrees
DLEDEG	ELEV_PCU_+	Elevator Deflection	degrees
DLADEG	AIL_PCU_+	Aileron Deflection	degrees
DLRDEG	RUDDER_POS	Rudder Deflection	degrees
MACH	MACH_A	Mach Number	Mach
EPR(1)	EPR_1	Engine Pressure Ratio #1	epr
EPR(2)	EPR_2	Engine Pressure Ratio #2	epr
ALT	BC_ALT1_A	Barometric Altitude	feet
PRESS	PS_CORR_A	Static Pressure	psf
TAS	TRU_ASPD_A	True Airspeed	knots
FNZ	++NORM_ACC_A	Normal Acceleration	ft/sec^2
TEMPRC	STAT_TMP_A	Static Temperature	^oC
DLGPCT	NOSE_GEAR	DOWN=1, UP=0	---
LONG_ACC_A	LONG_ACC_A	Longitudinal Acceleration	ft/sec^2
LAT_ACC_A	LAT_ACC_A	Lateral Acceleration	ft/sec^2
WEIGHT	+WEIGHT	Weight	lbs
WIND_SPD	WIND_SPD_A	Wind Speed	knots
WIND_DIR	WIND_DIR_A	Wind Direction	true degrees
E_VEL_IR_A	E_VEL_IR_A	E. Component of Velocity	knots
N_VEL_IR_A	N_VEL_IR_A	N. Component of Velocity	knots
VERT_SPD_A	VERT_SPD_A	Vert. Component of Velocity	ft/min
TRUE_HDG_A	TRUE_HDG_A	True Heading	degrees
PITCH ANGLE	PITCH_AT_A	Pitch Angle	degrees
ROLL ANGLE	ROLL_ATT_A	Bank Angle	degrees

* Refer to section 2.3